Universidade de Lisboa

Faculdade de Farmácia

Evaluation of chemically induced steatosis in different human *in vitro* hepatic systems

Tatiana Lopes Rodrigues

Mestrado Integrado em Ciências Farmacêuticas

2017

Universidade de Lisboa

Faculdade-de-Farmácia

Evaluation of chemically induced steatosis in different human *in vitro* hepatic systems

Tatiana Lopes Rodrigues

Monografia do Mestrado Integrado em Ciências Farmacêuticas apresentado à Faculdade de Farmácia da Universidade de Lisboa

Orientador: Robim M. Rodrigues, PhD e Tamara Vanhaecke, PhD

Co-orientador: Margarida F.B. Silva, PhD

2017

Com a colaboração da instituição:

Vrije Universiteit Brussel

Faculteit Geneeskunde en Farmacie

Acknowledgment

Ao finalizar esta caminhada de 5 anos fica um sentimento de gratidão imensa para com todos aqueles que tornaram este percurso possível de percorrer.

À minha família, obrigada por toda a confiança, apoio incondicional e palavras de orgulho transmitidos vezes sem conta. Obrigada mãe, avós, irmã e cunhado por me terem acompanhado de perto apesar da distância física.

Ao meu namorado, meu companheiro de aventuras, que nunca vacilou nos meus momentos de desespero e choradeira, obrigada pela tua paciência e companheirismo sem limites.

Às minhas amigas de faculdade, amigas para a vida, obrigada por terem partilhado esta caminhada comigo, sem vocês não teria sido tão cheia e marcante.

Por fim, não podia deixar de agradecer ao professor Robim Rodrigues, por me ter acolhido e integrado tão bem no departamento, por toda sabedoria transmitida e por todo o apoio concedido apesar de todos os compromissos que tinha. Obrigada também à professora Margarida Silva pelos conselhos e pela disponibilidade total prestados. Sem ambos, não teria sido possível elaborar uma monografia final tão rica e completa.

Tatiana Rodrigues

Outubro de 2017

Table of contents

Index of figures

Index of tables

Abbreviations

18S	18S ribosomal RNA
2-EH	2-Ethylhexanol
ACADs	Acyl-CoA dehydrogenases
ACC	Acetyl-CoA carboxylase
ACTB	Actin beta
ALT	Alanine aminotransferase
AST	Aspartate aminotransferase
Apo	Apolipoproteins
ApoB	Apolipoprotein B
ATGL	Adipose TG lipase
B2M	Beta-2 microglobulin
BMI	Body mass index
BMP	Bone morphogenic protein
CD36	Cluster of differentiation 36
ChREBP	Carbohydrate responsive element binding protein
CoA	Coenzyme-A
CPT	Carnitine palmitoyl transferase
CVD	Cardiovascular disease
DM2	Type 2 diabetes mellitus
DMEM	Dulbecco's Modified Eagle Medium
DMSO	Dimethyl sulfoxide
dNTPs	Deoxynucleotide triphosphates
DEPC	Diethylpyrocarbonate-treated water
FA	Fatty acids
FAS	Fatty acid synthase
FBS	Fetal bovine serum
FFA	Free fatty acids
FGF	Fibroblast growth factor
GAPDH	Glyceraldehyde 3-phosphate dehydrogenase
HBSS	Hanks’ Balanced Solution
HCC	Hepatocellular carcinoma
HGF	Hepatocyte growth factor
hiPSCs	Human-induced pluripotent stem cells

HMBS	Hydroxymethylbilane synthase
HNF	Hepatocyte nuclear factor
hSKP	Human skin-derived precursors
hSKP-HPC	hSKP derived hepatic progenitor cells
HSL	Hormone sensitive lipase
IC	Inhibitory concentration
ITS	Insulin transferrin sodium selenite
KLF4	Krüppel like factor 4
LCE	Long chain fatty acid elongase
LCFA	long chain fatty acids
L-PK	Pyruvate kinase
LPL	Lipoprotein lipase
MTP	Microsomal TG transfer protein
MTT	3-(4,5-dimethylthiazol-2-yl)-2,5-diphenyltetrazolium bromide
MYC	V-myc myelocytomatosis viral oncogene homolog
NAFLD	Non-alcoholic fatty liver disease
Na-OA	Sodium Oleate
NASH	Non-alcoholic steatohepatitis
Na-VPA	Sodium Valproate
NTC	Non-template control
OCT4	Octamer binding transcription factor 4
OSM	Oncostatin M
PBS	Phosphate buffered saline
PCR	Polymerase chain reaction
qPCR	Quantitative PCR
SCD1	Stearoyl-CoA desaturase 1
SOX2	Sex-determining region Y box 2
SREBP	Sterol regulatory element binding protein 1 c
SRY	Sex-determining region-Y
TCA	Tricarboxylic acid
Tet	Tetracycline
TG	Triglycerides
UBC	Ubiquitin C
VLDL	Very low-density lipoproteins

Abstract

Non-alcoholic fatty liver disease (NAFLD) is histologically defined by atypical accumulation of hepatic lipid droplets, known as hepatic steatosis. The increased accumulation of triglycerides in the liver is a result of an abnormal lipid metabolism reflected by a greater input (uptake and synthesis) than the fatty acids output rate (oxidation and secretion). During the last decades liver toxicity has been not only the leading cause for pharmacovigilance safety reports and the withdrawing of previously approved drugs but also one of the major causes of discontinuation of the development of new chemical entities. Therefore, the issue of drug induced steatosis should be addressed during preclinical drug development. Since robust human-relevant *in vitro* models are lacking, it is necessary to develop predictable culture systems in toxicity testing.

HepG2 cells are one of the most used *in vitro* models to study hepatotoxicity, however, this cell model has some limitations and does not fully represent the human hepatic metabolism nor the population diversity. On the other hand, stem cell-derived hepatic cells, such as human skin-derived precursors differentiated into hepatic cells (hSKP-HPC), are emerging as suitable *in vitro* study system for preclinical evaluation of hepatotoxic compounds.

The present research work aims to characterize these cell systems for the study of steatogenic compounds, namely a fatty acid (Sodium Oleate), two drugs (Tetracycline and Sodium Valproate) and a chemical solvent (2-ethyhexanol). The induced steatosis was evaluated in each *in vitro* model through the observation of intracellular accumulation of lipids and through the analysis of the expression of important genes involved in intracellular lipid accumulation.

Preliminary results revealed that hSKP-HPC was the cell model with highest accumulation of neutral lipids, followed by undifferentiated hSKP. Nonetheless, the obtained gene expression profiles were inconclusive, especially for hKSP-HPC. However, previous findings had already demonstrated the potential of hSKPs as a human relevant *in vitro* model to identify drug induced hepatotoxicity and future research work is needed.

Stem cell technology is still an expanding area with potential use in hepatic toxicity testing. Yet, issues such as disparities between cell cultures and hepatic differentiations still need to be overcome.

Keywords: NAFLD, steatosis, *in vitro* hepatic systems, stem cells

Resumo

A doença de fígado gordo não alcoólico (NAFLD) é definida histologicamente como a acumulação atípica de gotículas lipídicas hepáticas, conhecida por esteatose hepática. A acumulação de triglicéridos no fígado é resultado de um metabolismo lipídico anormal que é refletido por um desequilíbrio entre a absorção e síntese de ácidos gordos e a oxidação e secreção. Ao longo das últimas décadas, a toxicidade hepática tem sido não só a principal causa para a retirada de fármacos do mercado, mas também, um dos maiores motivos para a descontinuação do processo de desenvolvimento e investigação de novas moléculas candidatas a fármacos. Assim, a esteatose potencialmente induzida por fármacos deve ser estudada durante a fase pré-clínica de desenvolvimento de fármacos. Para cumprir esse objetivo, é necessário o desenvolvimento de sistemas robustos in vitro de cultura de células de origem humana para estudo da hepatotoxicidade de modo a preencher as lacunas existentes.

As células HepG2 são um dos modelos in vitro mais utilizados para estudar a hepatotoxicidade, contudo, este possui algumas limitações não representando o metabolismo hepático humano na sua globalidade nem a diversidade populacional. Por outro lado, células hepáticas diferenciadas de células estaminais, obtidas a partir de precursores derivados da pele humana (hSKP-HPC) têm vindo a emergir como um novo modelo in vitro para a avaliação pré-clínica de compostos que possam induzir esteatose.

Este trabalho experimental visa caracterizar estes modelos celulares na investigação de compostos esteatogénicos tais como: um ácido gordo (oleato de sódio), dois fármacos (tetraciclina e valproato de sódio) e um solvente químico (2-etilhexanol). A indução da esteatose foi avaliada em cada modelo celular através da observação da acumulação intracelular de lípidos e da análise da expressão génica de diversos genes importantes no mecanismo celular da esteatose.

Os resultados obtidos revelaram que as hSKP-HPC foram o modelo celular com maior acumulação lipídica. Contudo, os perfis de expressão génica observados foram inconclusivos. Ainda assim, estudos anteriores demonstraram o potencial das hSKP-HPC como um relevante modelo in vitro que permite a deteção de esteatose induzida por fármacos.

A tecnologia das células estaminais é ainda uma área em expansão com aplicabilidade no estudo da hepatotoxicidade hepática. Porém, existem ainda diversas incertezas relacionadas com disparidades entre culturas celulares e processos de diferenciação hepática e, por isso mesmo, futuro trabalho de investigação deverá ser feito.

Palavras-chave: NAFLD, esteatose, sistemas hepáticos in vitro, células estaminais

1. Introduction

1.1 Non-alcoholic fatty liver disease

In mammals, liver is a multifunctional organ that is responsible for controlling the metabolic homeostasis of glucose, lipids and proteins and is also involved in detoxification and nutrient storage. Dysregulation of any of these processes can lead to liver disease, specially to metabolic disorders that contribute to health detriment of individuals. In the case of non-alcoholic fatty liver disease (NAFLD), numerous derangements can be found in the liver´s capacity to process lipids. The ethology of the disease has been linked to external factors such as dietary habits or individual multifactorial alterations in genetics, adipose tissue, hormone regulation and the immune system. [1] [2]

1.1.1. Primary and secondary NAFLD

Insulin resistance as observed in overnutrition and obesity is known as "primary NAFLD". Besides these, other well-known risk factors of NAFLD are included in the definition of metabolic syndrome such as hyperinsulinism, type II diabetes mellitus, hypertriglyceridaemia, low levels of high-density lipoproteins, hypertension and accumulation of visceral fat. [3] [4] However, other less common conditions can cause a similar clinical and histologic picture, and these might enter into the differential diagnosis of secondary NAFLD in patients who do not have traditional risk factors. Some of those uncommon causes of secondary NAFLD are inborn errors of metabolism, total parenteral nutrition, surgical interventions (e.g. liver transplantation and jejunoileal bypass surgery), hepatitis C infection, celiac and Wilson disease, exposure to toxins and drugs, among others. [5]

1.1.2. Natural history of NAFLD

Over the last decades, the problem of obesity has grown tremendously and along with it, NAFLD has become an important health concern among patients without significant alcohol consumption[1]. NAFLD is the most common cause of liver disease worldwide and it might

[1] The cut-off limit of alcohol intake that distinguishes between alcoholic and non-alcoholic fatty liver disease is not known, although 20 g/day for women and 30 g/day for men are commonly used.

become a leading indication for liver transplantation in the future. [6][7] Clearly connected to the metabolic syndrome, this disease is histologically defined by increased hepatocellular storage of triglycerides (TG), known as hepatic steatosis. The presence of fat in liver parenchyma is called "steatosis" when the lipid deposition is found in >5% of hepatocytes or "fatty liver" when it involves more than 50% of hepatocytes. [8] The spectrum of NAFLD ranges from simple steatosis to non-alcoholic steatohepatitis (NASH), fibrosis, cirrhosis and finally hepatocellular carcinoma (HCC) *(Figure 1.1*). NASH is defined as steatosis in the presence of hepatocellular injury, hepatocyte ballooning, lobular inflammation and subsequent scarring and replacement of the tissue with type I collagen. Whereas approximately 38% of patients with NASH develops fibrosis and cirrhosis within a 10 year period or even hepatocellular carcinoma, the SS has a relatively favourable clinical course and rarely progresses to advanced disease. NAFLD is strongly associated with insulin resistance that is considered a hepatic manifestation of metabolic syndrome and is related with oxidative stress, abnormal production of cytokines and deregulation of fatty acids (FA) metabolism. Besides that, this disease is considered a risk factor for type 2 diabetes mellitus (DM2), dyslipidemia and cardiovascular disease (CVD). For that reason, NAFLD increases the risk of mortality not only from liver disease but also from non-liver related causes such as malignancy, diabetes and CVD. [9]

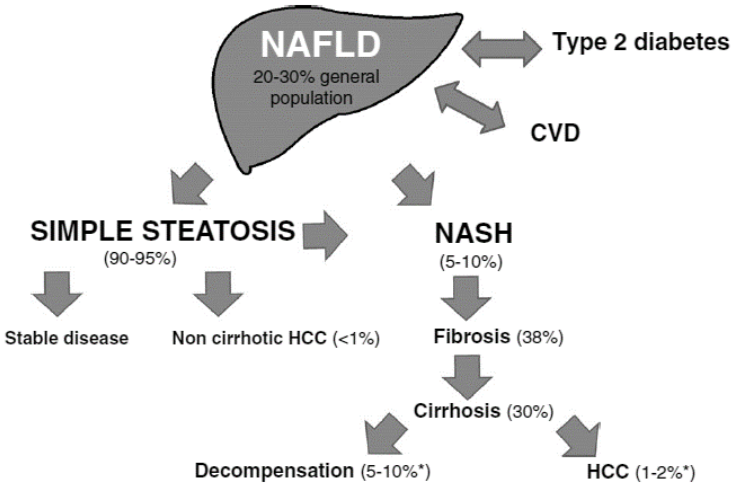

***Figure 1.1* – Natural history of NAFLD and respective incidence**. Among 20-30% of general population has NAFLD and CVD and DM2 are important risk factors. The majority of the NAFLD population develop simple steatosis, which is not associated with impaired survival. Only 5–10% of patients diagnosed with NAFLD will develop NASH and 30% of these well develop cirrhosis. In 10 years from development of cirrhosis, 1-2% of patients will develop HCC. Adapted from Buzzetti et al. 2016 [10]

1.1.3. Diagnosis of NAFLD

Patients with non-alcoholic fatty liver disease are commonly asymptomatic and, when present, manifest nonspecific symptoms such as fatigue and abdominal discomfort. The diagnosis should be considered after exclusion of other causes of liver disease in patients with abnormal liver tests and with the presence of metabolic risk factors. The Fibrosis Score which incorporates age, body mass index (BMI), AST/ALT ratio (aspartate aminotransferase and alanine aminotransferase, respectively), platelet count and albumin is a non-invasive scoring model to assess fibrosis in NAFLD. Ultrasound is another diagnostic tool that has a great level of sensitivity when steatosis is greater than 30%. Magnetic resonance spectroscopy is more sensitive but has limited availability since it is an expensive method. Nowadays, liver biopsy still represents the gold standard for the diagnosis of NAFLD/NASH as it serves as the only means of distinguishing steatosis from steatohepatitis. [2,7]

1.1.4. Treatment of NAFLD

When it comes to the treatment of NAFLD, a multifactorial approach is needed so that the focus should be on the disease as well as on metabolic comorbidities. For all NAFLD patients, lifestyle interventions are crucial and must be recommended as a first line measure. Weight management through improvements in diet and increased physical activity can not only improve liver histology but also delay disease progression. [11][12] When lifestyle interventions are not effective, a pharmacological treatment must be considered although practice guidelines recommend pharmacologic intervention only in patients with NASH. Given the importance of insulin resistance in NAFLD, insulin sensitizers such as metformin, thiazolidinedione and incretins have been studied. Additionally, the use of lipid lowering drugs like statins, fibrates and omega-3 polyunsaturated fatty acids are also used to control the dyslipidaemia. Other important drugs that might be helpful in the pharmacological management of NAFLD are antihypertensive agents such as angiotensin II receptor blockers and anti-oxidants such as vitamin E and pentoxifylline that is also cytoprotective and anti-inflammatory. A large number of drugs are currently under investigation or in development, but at present there is no specific therapeutic agent approved by regulatory agencies therefore their use is off-label. [8][12]

1.1.5. Molecular mechanisms in NAFLD

The “two hit hypotheses” proposed in 1998 by Day and James provides a pathophysiologic rationale for the progression of steatohepatitis. The first hit reflects the reversible accumulation of TG and free fatty acids (FFA) and primes the cells to the second hit that involves lipid peroxidation, mitochondrial dysfunction and inflammation. Those events lead to NASH, which is defined by the presence of cytokine-induced hepatocyte damage and liver fibrosis. [13]

Nowadays, this theory is obsolete and the “multiple-hit” hypothesis appeared to explain NAFLD pathogenesis and its multiple insults. Such hits include genetic factors, insulin resistance, hormones secreted from the adipose tissue, obesity and changes in gut microbiome. Consequently, the energy homeostasis will be compromised and the overflow of FFA in the liver may result in endoplasmic reticulum stress, mitochondrial dysfunction and consequent activation of inflammatory responses. [10]

The increased accumulation of TG in the liver develops when the rate of FA input (uptake and synthesis) is greater than the rate of FA output (oxidation and secretion). Therefore, steatosis can result from multiple factors such as:

1- Increased lipolysis and increased FA uptake from diet
2- Mitochondrial dysfunction that results in reduced FA oxidation
3- Increased *de novo* lipogenesis
4- Reduced lipid clearance that is reflected by reduced very low-density lipoprotein (VLDL) secretion

These mechanisms will be discussed in the next subchapters and are summarized in *Figure 1.2.*

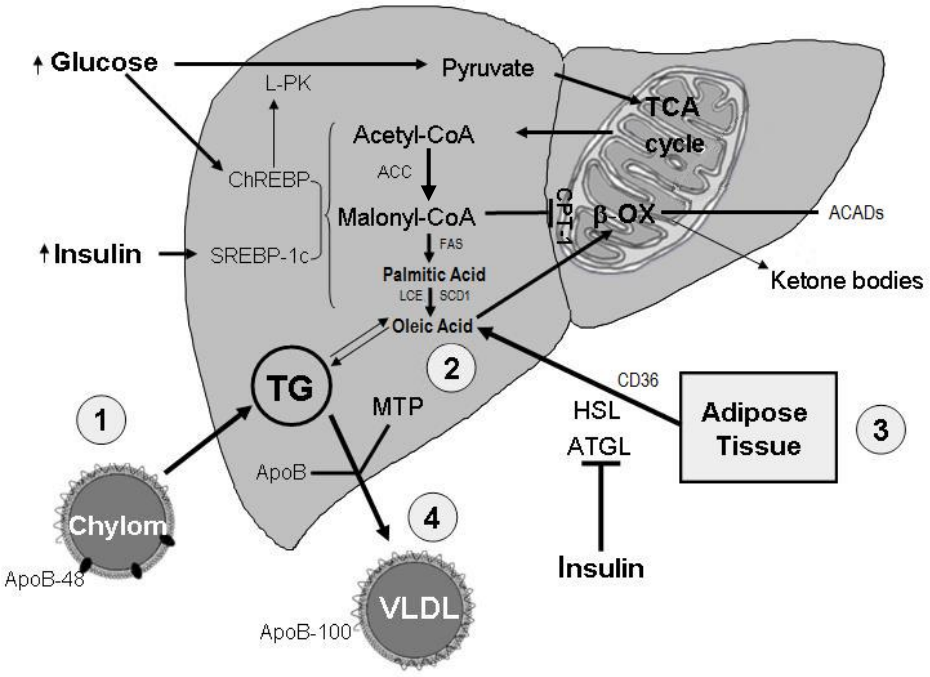

***Figure 1.2* – Hepatic triglyceride metabolism**. FAs can be obtained by three major sources: ① diet, through the uptake of dietary fats that are transported by chylomicra; ② endogenous synthesis, through *de novo* lipogenesis; and ③ peripheral tissues, especially adipose tissue via lipolysis and transport protein *CD36*. The ingestion of carbohydrate increases glucose, a substrate of *de novo* lipogenesis, that activates the transcription factor ChREBP. On the other hand, insulin is also increased with the ingestion of carbohydrate which leads to the activation of SREBP-1c. Both ChREBP and SREBP-1c will activate other lipogenic genes such as *ACC* and *FASN*. Simultaneously, hyperglycemia activates ChREBP which increases the expression of L-PK that will convert glucose into pyruvate enabling the initiation of the Krebs cycle. The synergic actions of SREBP-1c and ChREBP up-regulate the enzymatic machinery for the conversion of excess glucose into FA obtaining palmitic acid that is desaturated by *SCD1* to form oleic acid. The FA can be used to synthesize triglycerides that can be conjugated with ApoB into VLDL and secreted into blood ④. Increased *de novo* lipogenesis results in increased levels of malonyl-CoA which inhibits CPT-1, the protein responsible for internalization of LCFA into the mitochondria, and consequently reduces the β-oxidation process. Adapted from Donato et. Al 2012 [14]

1.1.5.1. Fatty acids uptake

The FFA used for hepatic formation of TG by esterification are derived from several sources: diet, adipose tissue or peripheral tissues and *de novo* synthesis.

During the feeding state, dietary fats are emulsified by bile acids, hydrolysed, absorbed and resynthesized by the enterocytes as TG-rich chylomicra. These are transported by blood to the peripheral organs, via the circulatory system as apolipoproteins, such as ApoB-48. About 20% of the chylomicra are delivered to the liver where they are hydrolysed to FA by the lipoprotein lipase (LPL).

During fasting conditions, the major source of FFA delivered to the liver is generated by adipose tissue via lipolysis. Hormone sensitive lipase (HSL) and adipose TG lipase (ATGL) are essential enzymes for the initial steps of the hydrolysis of stored TG into FFA. The activity of these enzymes is promoted by catecholamines, natriuretic peptides and glucagon, and is repressed by insulin under feeding conditions. [15] [14]

The rate of FA uptake depends not only on the FA concentration in the plasma but also on the number and activity of transporter proteins on the membrane of the hepatocytes. Also known as fatty acid translocase, the cluster of differentiation 36 (CD36) is a well-known transmembrane transporter protein that facilitates the uptake and intracellular trafficking of FFA and whose expression is enhanced in NAFLD patients. [1] [16] [17]

High-fat diets are one major contributing factor cause of steatosis. In addition to the increased uptake of lipids, the insulin resistance (IR) state that is frequently associated with obesity, goes along with increased adipocyte lipolysis, leading to higher levels of FFA in the plasma independently from the nutritional status. [18]

1.1.5.2. *De novo* lipogenesis

De novo lipogenesis is the process in which the liver synthesizes endogenous FA through a metabolic pathway that involves glycolysis, biosynthesis of saturated FAs followed by desaturation, and the formation of TG. Firstly, glucose is hydrolysed into pyruvate through pyruvate kinase (L-PK) which is then converted to acetyl-coenzyme A (acetyl-CoA) in the mitochondria entering the tricarboxylic acid or Krebs cycle. In the cytosol, the acetyl-CoA is carboxylated by Acetyl-CoA carboxylase (ACC) to malonyl-CoA, a key molecule in controlling the intracellular anabolic or catabolic FA pathways. To form one palmitate molecule, several cycles of metabolic reactions are needed. Fatty acid synthase (FAS), which is encoded by *FASN* gene, catalyses the formation of palmitic acid (a 16-carbon fatty acid) from malonyl-CoA. Palmitic acid is then elongated by the long chain fatty acid elongase (LCE) and desaturated by stearoyl-CoA desaturase 1 (*SCD1*) to form oleic acid (an 18-carbon unsaturated fatty acid). These fatty acids are hepatic lipid metabolism regulators and are used to synthesize TG that are the primary source of energy storage and transport. [17] [19]

The rate of *de novo* lipogenesis is regulated primarily at the transcriptional level. Glucose and insulin levels, that are influenced by hormonal and dietary conditions, promote lipogenesis by

activation of hepatic transcription factors. Hyperglycaemia increases lipogenesis by activating the transcription factor carbohydrate-responsive element-binding protein (ChREBP). ChREBP expression activates L-PK, thus providing a substrate for FA, and subsequently TG synthesis for storage and release. Insulin stimulates transcription factor sterol regulatory element-binding protein- 1 c (SREBP – 1c) which up-regulates the expression of lipogenic genes, including *FAS*, *ACC* and *SCD1*. [17] [20]

NAFLD has been associated with high levels of insulin and glucose and consequently with increased hepatic expression of these transcriptional factors that leads to hepatic TGs accumulation in lipid droplets known as steatosis. [16]

1.1.5.3. Fatty acid β–oxidation

The oxidation of intrahepatocellular FA, which is critical for production of both ATP and ketone bodies, occurs primarily within mitochondria, and to a much lesser extent in peroxisomes and microsomes. FA β–oxidation is a process to shorten the FAs into acetyl-CoA. Short and medium chain FAs pass the mitochondrial membrane as free acids but long chain FAs (LCFA) are shuttled across the membrane trough carnitine palmitoyl transferase-1 (CPT1), also known as CPT1A.

For the translocation into intermembrane space, fatty acyl-CoAs (the activated form of fatty acids) are converted to fatty acyl-carnitines by CPT1 in the mitochondrial outer membrane. Long-chain acyl-carnitine represent the transportable form of activated FAs. After being transported across the mitochondrial outer membrane, fatty acyl-carnitines are again converted to fatty acyl-CoAs by CPT2 in the inner mitochondrial membrane. Inside the mitochondrial matrix, the acyl-CoA esters are dehydrogenated by acyl-CoA dehydrogenases (ACADs), a class of enzymes that is classified as short, medium or long according to its substrate. The formed acetyl-CoA units can be later converted into ketone bodies or can be incorporated into the TCA cycle for full oxidation and consequently production of ATP. [1][16][17]

Malonyl-CoA, an early intermediate of *de novo* lipogenesis produced during the postprandial state, inhibits CPT-1 and the entry of FAs into the mitochondria, hence reducing β-oxidation and increasing FA and TG accumulation. On the other hand, under fasting conditions, FA β-oxidation is enhanced via inactivation of ACC, resulting in the reduced production of malonyl-

CoA which will increase FA entry to mitochondria since the inhibition of CPT1 is supressed. [14]

In NAFLD patients, impaired ATP production and a decreased rate of FA oxidation were observed. [17]

1.1.5.4. Lipid secretion

Besides being oxidised in the mitochondria or re-esterified into TG and stored in lipid droplets, the FAs in the liver can also be coupled with apolipoproteins and secreted as constituents of very low-density proteins (VLDL). VLDL constitution is a hydrophobic core containing TG and cholesteryl esters and hydrophilic coating which consists phospholipids and apolipoprotein B (ApoB) 100, that is liver-specific. Their biosynthesis and maturation takes place in the endoplasmic reticulum and in the Golgi and is dependent of ApoB and microsomal TG transfer protein (MTP) which is responsible for the lipidation of ApoB with TG. The FA that are esterified into TG and secreted as VLDL are then exported from the liver and delivered to peripheral tissues. The VLDL secretion rate is limited by the availability of hepatic TG and the overall capacity for VLDL assembly. The regulation and assembly of VLDL is made by insulin. In response to this hormone, ApoB 100 is degraded by autophagy and the expression of MTP is negatively regulated. [17][18]

In NAFLD in the presence of insulin resistance, this process is enhanced due to increased *de novo* lipogenesis plus lipolysis of intrahepatic and intra-abdominal fat which results in hypertriglyceridemia and hepatic steatosis. Although TG secretion and production of VLDL might be increased, it cannot keep up with the increased rate of TG synthesis leading to excessive lipid accumulation in liver. [1]

1.2. Steatogenic compounds

As previously mentioned, NAFLD can result from steatosis induced by diet, drugs and chemicals. In order to mimic all situations, four different compounds capable of inducing steatosis were used.

1.2.1. Sodium Oleate (Na-OA)

Monounsaturated omega-9 oleic acid (C18:1) is the most abundant FA in nature and in diet. Besides this, is commercially used in the preparation of lotions, and as a pharmaceutical solvent. As shown in *Figure 1.2,* Na-OA is an end-product of *de novo* FA synthesis and contributes to the accumulation of TG in the liver. [21][22]

Na-OA was tested in order to mimic steatosis induced by a high-fat content diet.

1.2.2. Tetracycline (Tet)

Tetracycline is an antibiotic that inhibits protein synthesis and exhibits activity against a wide range of microorganisms. Due to its favourable antimicrobial properties and the absence of major adverse side effects, this agent is extensively used in the therapy of human and animal infections. [23] Large intravenous doses of tetracycline may induce microvesicular steatosis which is described as diffuse accumulation of small fat droplets without evidence of significant inflammation. This process is associated with several mechanisms such as inhibition of the mitochondrial respiratory chain decreasing FA β-oxidation, inhibition of MTP activity which decreases lipoprotein export and increase of *de novo* lipogenesis. In addition, it was demonstrated that Tet upregulated the expression of CD36 in HepG2 and in mouse and that facilitates hepatic FA uptake and esterification to TG. [24][25]

1.2.3. Sodium Valproate (Na-VPA)

Sodium valproate is a branched short-chain FA used mainly as an anticonvulsant and mood stabilizing drug. Like tetracycline, valproic acid induces microvesicular steatosis by inhibiting mitochondrial enzymes involved in β-oxidation and in TG secretion (MTP) and sequestering of essential cofactors for the esterification of FAs such as coenzyme A. [26] [27]

Both Tet and Na-VPA were tested to mimic drug induced steatosis.

1.2.4. 2-Ethylhexanol (2-EH)

2-Ethylhexanol is an alcohol poorly soluble in water produced on a massive scale for use in numerous applications in the cosmetic and chemical industry. It is used as a low volatility solvent for resins, animal fat, vegetable oils, insecticidal sprays, among others. Due to its characteristic floral fragrance is present in perfumes, shampoos and detergents. However, its main use is as a precursor for the synthesis of phthalate plasticizers, coatings and other

speciality chemicals. It has been described that prolonged exposure to this solvent might induce steatosis by inhibiting mitochondrial β-oxidation. [28][29]
2-EH was chosen in order to mimic industrial chemical induced steatosis.

1.3. Hepatic Cell Models Study Systems

1.3.1. Overview: toxicology and pharmaceutical industry

It takes 10-15 years to develop a new drug from its discovery to regulatory approval. Studies indicate that only 5 of every 10 000 compounds explored will reach clinical trials stage and of those that get approved, only 20-30% of the drugs recover their fully investment. The cost of developing drugs is increasing which puts additional pressure on pharmaceutical industry. Attrition rates are very high, for instance a candidate drug have only 22% chance of completing clinical development. This add enormous strain on new drug development since monetary investments and resources are being occupied and wasted. A large number of compounds fail in later development stages due to unexpected toxicities. This represents a serious issue to be addressed by pharmaceutical companies.

In addition, during the last decades liver toxicity has been the leading cause for pharmacovigilance safety reports and the withdrawing of previously approved drugs. Drug induced hepatotoxicity, including drug induced steatosis that could lead to liver failure, is another significant problem that concerns pharmaceutical industry. Since the development of new drugs is a complex, lengthy and very expensive process, it is crucial to screen low-toxicity drug candidates and to rule out the drugs that are able to induce liver injury in early developmental stages. [30][31][32]

The gold standard for hepatic safety testing is *in vivo* screening for hepatotoxicity during pre-clinical and clinical phases of the development. On the one hand, this methodology raises a lot of ethical issues and concerns about animal welfare. On the other hand, is time consuming, expensive and inaccurate since among 38% and 51% of compounds showing liver effects in humans do not present those effects in animals. In addition, *in vivo* studies cannot evaluate the much lower concentrations and mixtures of chemicals that humans are exposed to, lack information regarding mechanisms of actions and cannot account for human variability in responses and susceptibility. The 3R policy (Refinement, Reduction, Replacement) has been

introduced worldwide and calls for the use of alternative methods to animal testing whenever possible. [32][33]

It is crucial to develop effective *in vitro* culture systems in toxicity testing. The use of *in vitro* model systems has many advantages such as: the decrease in number and animals; the reduced cost of animal maintenance and care; the reduction of the time needed to obtain results; the decrease in quantity of chemical needed; the possibility to include a greater number of chemicals and chemicals mixtures and to study chemical metabolism, mechanisms of toxicity and dose-response relationships. [34][33]

1.3.2. Primary hepatocytes

Fresh primary human hepatocytes have been the gold standard for *in vitro* testing since they express various drug metabolizing enzymes at comparable levels to those found *in vivo.* These cells are used to study the effects of long-term toxicant exposure, to examine inter-individual differences in xenobiotic metabolism and to characterize drug induced toxicities *in vitro.*

The hepatocytes are isolated by collagenase digestion and during this complex process some of the hepatocyte-specific characteristics are lost. Response to chemical exposures can be different than those occurring *in vivo* because cells have lost their microenvironment structure, cell to cell interactions and cell membrane structures.

Primary cultures are less homogeneous than cell lines and exhibit inter-individual variations in drug metabolizing profile. Also, the availability of freshly prepared primary human hepatocytes due to intensified liver transplantation programs and their high cost are another limitation. In addition, the maintenance of liver-specific functions such as albumin production and cytochrome P450 expression depends on optimal growth conditions, cell culture format and matrix composition. Therefore, the human hepatocytes are phenotypically unstable and have a limited life span. [34][35][36]

1.3.3. Hepatic cell lines

A cell line is a permanently established, transformed clonal lineage, where the daughter cells will proliferate indefinitely when given proper medium and growth conditions. Due to

mutations in growth control pathways, cells lines are not restricted to a limited number of cell divisions. Human cell lines are a cheaper and available alternative than human hepatocytes. In addition, these cell lines grow steadily, have simpler culture conditions, have almost an unlimited life-span and have a stable phenotype which increases reproducibility. Unfortunately, the cells do not possess the full range of phenotypic characteristics of the liver tissue like hepatocyte cultures and are usually obtained from tumours. [37][33]
Although there is a wide range of hepatic cell lines, only HepG2 were used to perform the experiments.

1.3.3.1. HepG2

The Hep G2 line was generated in the 1970s derived from a well-differentiated hepatocellular carcinoma and expresses many liver-specific genes. They are adherent, epithelial-like cells easy to maintain and grown as monolayers and in small aggregates. There is a vast collective knowledge about how these cells behave and respond under specified conditions which is a great advantage when doing mechanistic studies. However, their metabolic activity is lower than primary hepatocytes and the expression profile of phase I and phase II enzymes has been shown to vary between passages. In addition, this cell line does not represent population diversity. Yet, HepG2 cells represent the most widely employed hepatic *in vitro* model in hepatotoxicity testing by pharmaceutical industry. [30][33]

1.3.4. Stem cells

Stem cells are undifferentiated cells capable of extensive self-renewal through cell division, while maintaining the capacity to differentiate into tissue- or organ-specific cells under appropriate conditions. Therefore, stem cells represent a renewable source of cells that can be grown up in large scale thus providing a large number of functionally equivalent cells that could be stored for later use. For those reasons, these cells are a novel and attractive alternative human cell source that can be used as *in vitro* model for toxicology studies. [30][36]

Stem cells are distinguished by their developmental status and differentiation potential and are therefore often classified as pluripotent (embryonic stem cells and induced pluripotent stem cells) or multipotent (adult stem cells).

1.3.4.1. Embryonic stem cells

The totipotent fertilized egg is the ultimate stem cell that originates the developing embryo and their adjacent structures. Embryonic stem cells are pluripotent cells derived from the inner cell mass of blastocysts (embryoblast) that are capable of nearly unlimited self-renewal. These cells retain the ability to differentiate into every cell type from each of the three germ layers: endoderm, mesoderm and ectoderm. Under normal circumstances, pluripotent stem cells are not present in the adult organism thus human embryonic stem cells are extracted and isolated from the embryoblast to produce continuous cell lines. [38][39]

1.3.4.2. Human induced pluripotent stem cells (hiPSCs)

Reprogramming somatic cells is an innovating way to obtain pluripotent stem cells avoiding the ethical issues related with the use of embryonic stem cells. Human induced pluripotent cells are generated by reprogramming somatic cells through the overexpression of several transcription factors: Krüppel-like factor 4 (KLF4), octamer binding transcription factor 4 (OCT4), SRY (sex determining region Y)-box 2 (SOX2) and v-myc myelocytomatosis viral oncogene homolog (MYC). However, the differentiation of hiPSCs into hepatocyte-like cells through retroviral reprogramming, without genetic and epigenetic abnormalities that could restrict the genetic expression pattern, might be a challenge. To overcome this drawback, new alternative methods to generate hiPSCs using synthesized RNAs and proteins are emerging. [40][41][42]

1.3.4.3. Adult stem cells

Adult stem cells, which exist in the postnatal organism, are either multipotent or unipotent meaning that they can both self-renew and differentiate to form some or all the cell types in specific tissues or organs. However, unlike embryonic cells, their lifecycle is limited to a maximum of fifty cell divisions. These cells have also the capacity to assist in repair and regeneration of the tissue or organ within they reside. [33][43]

The restricted locations where the cells reside are called stem cell niches that, under an inductive microenvironment enriched by regulatory signalling molecules, guide cell self-renewal and differentiation. [44] Those niches can be found in a wide range of tissues such as bone marrow,

adipose tissue, neuronal tissue, liver, intestinal crypt, umbilical cord matrix umbilical cord epithelial cell layer and placenta.[38][45][36]

Human skin-derived precursors (hSKP) are a multipotent cell population isolated from mammalian dermis obtained from skin biopsies of the abdomen, foreskin, breast, arm, face and scalp. These cells can be differentiated into a hepatic lineage after the sequential exposure to growth factors and cytokines that mimic liver development *in vivo*. Since human skin is a very accessible human tissue this is a potential novel *in vitro* model for hepatotoxicity screening of chemical substances. [36][46]

1.3.4.4. Differentiation of human stem cells

Besides somatic reprogramming, directed differentiation is another way to generate human target cells, in this case hepatocyte-like cells. When a developing embryo produces a particular cell type, the micro-environment is very dynamic with sequential biological events that stimulate the specification, differentiation and maturation of stem cells into a specific somatic cell. The identification of those *in vivo* intra- and extracellular signalling patterns is vital to induce the *in vitro* differentiation into a specific cell line. Most approaches are based on:

- Addition of soluble medium factors (growth factors, cytokines, corticosteroids, hormones) in a time-specific sequential manner to optimize the differentiation. The most essential extracellular signals are activin A, fibroblast growth factor (FGF), bone morphogenic protein (BMP), hepatocyte growth factor (HGF), oncostatin M (OSM), insulin-transferrin-sodium-selenite (ITS) and dexamethasone.
- Reconstruction of cell-matrix with natural scaffold collagen and cell-cell interactions.
- Determination of cell fate via genetic modification with liver-enriched transcription factors such as hepatocyte nuclear factor (HNF).

The ultimate goal is to obtain cells with morphological, phenotypic, and functional characteristics of hepatocytes that could be used as a predictive human-based cell system for hepatotoxicity screening of drugs. Despite great prospective, there are still hurdles to overcome when it comes to the application of these cells in toxicology. The incomplete understanding of *in vivo* mechanisms that drive cell differentiation and the absence of standardization represent issues yet to address. [41][44][47]

2. Objectives

The aim of this study is to investigate the molecular mechanisms involved in steatosis induced by compounds that mimic different causes of this disease, using human-based hepatic *in vitro* models. Hereby hepatic cell models are exposed to (i) compounds that mimic a high fat-diet, (ii) steatogenic drugs and (iii) industrial chemicals known to cause fatty liver.

To observe the accumulation of hepatic lipids (steatosis), three different human *in vitro* hepatic systems were used such as an immortalized hepatic cell line (HepG2) and hepatic differentiated and undifferentiated human skin-derived precursors (hSKP-HPCs and hSKPs).

The steatosis was induced by incubation of the three *in vitro* models with four steatogenic compounds known in literature for inducing lipid accumulation in the liver and with defined sub-cytotoxic concentrations. Sodium oleate (Na-OA) simulates a high fat diet situation. Exposure to two steatogenic pharmaceutical drugs [Tetracycline (Tet) and Sodium Valproate (Na-VPA)] is carried out as a representation of drug-induced steatosis. Finally, exposure to 2-ethylhexanol (2-EH), which has been associated with fatty liver induction, represents chemically-induced steatosis.

After the incubation period, the induced steatosis was evaluated in each *in vitro* model at a phenotypic level, through the observation of intracellular accumulation of lipids and at a molecular level, through the analysis of the expression of specific genes involved in the molecular mechanisms characteristic of the onset of the disease. The techniques that were involved in the experimental work were cytochemical staining of neutral lipid droplets and the quantitative polymerase chain reaction (qPCR), respectively. The gene *CD36* was used to represent fatty acid uptake, the *FASN* and *SCD1* to represent *de novo* lipogenesis, *ACADSB* and *CPT1A* to represent β-oxidation and *APOB* to represent triglyceride secretion.

The final purpose of this investigation is to evaluate the applicability of a novel *in vitro* hepatic cell system (HPC-hSKPs) to predict drug toxicity, more specifically hepatic steatosis.

3. Materials and Methods

3.1. Cell cultures

3.1.1. Freezing cells

In order to keep the cells for long periods of time, they are cryopreserved in liquid nitrogen at the temperature of -196°C. Each vial of 1 mL contains a cryoprotectant solution composed of 90% (v/v) of medium containing fetal bovine serum (FBS) and 10% (v/v) of dimethyl sulfoxide (DMSO). Before being transferred to the liquid nitrogen, the vials are appropriately labelled and stored for 24h at -80°C in an isopropanol recipient (Mr Frosty) that allows the cells to freeze slowly and avoid crystals formation. This freezing container is designed to achieve a rate of cooling of -1°C/min which is an optimal rate for cell preservation.

3.1.2. Thawing cells

As opposed to the freezing process, the cells should be thawed quickly by putting the vials into a water bath at 37°C. The vials cover should not touch the water and the vial must be kept in the bath the minimum time as possible.

To obtain a DMSO concentration that does not exceed 0.5% (v/v) of DMSO per T75 culture flask (T75cm^2), the content of the vial must be re-suspended in 20 mL of pre-warmed culture medium.

1 vial = 10% (v/v) DMSO = 0.1 mL DMSO

0.1 mL DMSO/20 mL culture medium = 0.5% (v/v) of DMSO

Considering the growth rate of each cell type and the desirable confluence that we wanted to obtain, 1 vial was used per T75 flask with HepG2 cells and 2 vials were used per T75 with hSKPs.
The media must be changed on the following day and the amount of 10 mL must be added since the DMSO is already diluted. In the specific case of the hSKPs cells, the wash medium must always be enriched with 20% of B27, a supplement composed by antioxidants and insulin.

As an alternative and, to remove 100% of the cryoprotectant, the vial can be re-suspended in 25 mL of pre-warmed culture medium and centrifuged for 5 minutes at 1200 rpm. The supernatant media is carefully removed and the cell pellet is homogenised with 1mL culture

medium. The suspension is transferred to a T75 culture flask with 10 mL of culture medium. The media must be changed on the following day.

The HepG2 and both differentiated and undifferentiated human skin-derived precursors (hSKP) cells grown as a monolayer in 75 cm^2 tissue culture flasks (Falcon) at 37°C ± 1°C, 90% ± 5% humidity and 5% ± 1% CO_2 in an incubator.

After thawing, the cells were passaged at sub confluence at least three times before use in exposure experiments and the medium was refreshed every 2-3 days.

3.1.3. Culture medium

HepG2

The culture medium of HepG2 for routine culture is composed of Dulbecco's Modified Eagle Medium (DMEM, by Lonza) with L-glutamine and high glucose (4.5mg/L) supplemented with 10% (v/v) of FBS and 100µg/mL of Penicillin/Streptomycin stock solution.

For 500mL of culture medium:

- 445mL of DMEM
- 50mL of FBS
- 5mL of Pen/Step stock solution

hSKP

When working with differentiated and undifferentiated hSKP cells different types of medium must be used.

The hSKP wash medium is used after the hSKP isolation, in the spheres formation process, and in the growth of undifferentiated hSKP cells. This hSKP wash medium is composed of Dulbecco's Modified Eagle Medium (DMEM) (Gibco by Life Technologies™) + GLUTAMAX™ with F12 nutrient mix (Gibco by Life Technologies™) (3:1), 1% of Streptomycin sulphate (50µg/mL), 1% of Benzyl Penincilin (7.33IU/mL) and 1% of Fungizone (2.5 µg/mL) (amphotericin B, Gibco by Life Technologies™).

For 500mL of culture medium:

- 367.5mL of DMEM + GLUTAMAX
- 122.5mL of F12 Nutrient mixture
- 5mL of Streptomycin sulphate
- 5mL of Benzyl Penincilin
- 5mL of Fungizone

The hSKP Basal Medium is used throughout the differentiation process and contains, additionally to the wash medium composition, L-Ascorbic Acid (0.1mM), Nicotinamide (4mg/mL), Linoleic acid-albumin (1mg/mL) and Sodium Pyruvate (27.3mg/L) (all from Invitrogen).

For 500mL of culture medium:

- 367.5mL of DMEM + GLUTAMAX
- 122.5mL of F12 Nutrient mixture
- 5mL of Streptomycin sulphate
- 5mL of Benzyl Penincilin
- 5mL of Fungizone
- 5mL of L-Ascorbic Acid
- 2mL of Nicotinamide
- 5mL of Linoleic acid-albumin
- 500µL of Sodium Pyruvate

3.1.4. Subculture of cells

When cells exceed 50% confluence (but are less than 80% confluent) they should be removed from the flask by trypsinization so that the cell death is avoided. Subculturing involves the removal of the medium and the washing of the cells with 10mL of phosphate-buffered saline (PBS) without Ca^{2+} and Mg^{2+} to remove any remaining serum that might inhibit the action of trypsin. The washing solution must be discard and 5 mL of Tryple Solution (Tryple™ Express Enzyme, by Life Technologies) must be added to the monolayer and then the cells are incubated at 37°C for a few minutes (3-4 minutes). Tryple™ Express is an animal origin-free recombinant enzyme used for dissociating the adherent cells by cleaving the peptide bonds of proteins on the C-terminal sides of lysine and arginine that facilitate cell-cell adhesion and adhesion of cells to the growth support surfaces. After the incubation time the flasks were gently tapped to detach the cells into a single cell suspension and the flask was washed with 20mL of media that were

collected into a 50mL tube. After 6 minutes of centrifugation at 1200rpm (335G) the obtained pellet was re-suspended in 1 mL of medium culture and viable cells were counted in a TC10^{TM} automated cell counter (Bio-Rad® by Life Science) by adding 10µL of Trypan Blue dye (Bio-Rad®) to 10µL of the obtained cell suspension. According to the cell count, a specific volume of cell suspension was redistributed in T75 culture flasks or 24 microwell plates (Falcon). The cell suspension was homogenized by cross agitation both in the flow and in the incubator.

When working with hKSPs, the washing step with PBS proved not to be advantageous so that the Tryple Solution must be added directly to the flask after the medium removal. Also, the wash medium must be enriched with 20% of B27 supplement and 5% of FBS (7.5 mL of wash medium, 2mL of B27 and 0.5mL of FBS). The FBS will facilitate the cells adherence to the flask and should be removed on the next day to ensure the cytoplasmic integrity and cells stability, by refreshing the medium with 8 mL of wash medium and 2mL of B27.

3.1.5. Cells seeding

A seeding density of approximately 13.000 cells/cm^2 (≈ 1×10^{6}cells/T75) was employed each time and according to the cells count or their confluent state a dilution rate (1/3, 1/4 or 1/5) was employed.

For example, with a cell count of 4×10^6 cells/mL the dilution rate should be 1/4.

4×10^6 cells → 1 mL cell suspension
1 T75 → 75cm^2×4 = 300cm^2 → available area to seed

Seeding on a T75

4×10^6 cells --------- 300cm^2
X cells ---------- 75cm^2
X= 1×10^{6}cells/T75

1 mL cell suspension ------- 300cm^2
X mL cell suspension ------- 75cm^2
X= 250µL cell suspension

1 T75: 250µL cell suspension + 10mL media

Seeding on a 24 microwell plate

1 well: 2 cm^2 → 24 wells: 48cm^2

4×10^6 cells --------- 300cm^2
X cells ---------- 48cm^2
X= $6,4\times10^5$cells/24 microwell plate

1 mL cell suspension ------- 300cm^2
X mL cell suspension ------- 48cm^2
X= 160µL cell suspension

1 24 microwell plate: 160µL cell suspension + 12mL media (500µL per well)

Seeding on a 96 microwell plate

1 well: 0,32 cm^2 → 60 wells (internal wells): 19.2cm^2

4×10^6 cells --------- 300cm^2
X cells ---------- 19,2cm^2
X= $2,56\times10^5$cells/24 microwell plate

1 mL cell suspension ------- 300cm^2
X mL cell suspension ------- 19.2cm^2
X= 64µL cell suspension

1 96 microwell plate: 64µL cell suspension + 6mL media (100µL per well)

3.2. Isolation of human skin-derived stem cells

The procedure used to isolate and subcultivate hSKP was previously described by Jeffrey A Biernaskie and his co-workers in 2006. [48] hSKP were isolated from small skin segments obtained by circumcision of boys between 2 and 10-year-old. Informed consent of the parents of the donors was obtained under the auspices of the Ethics Committee of the 'Vrije Universiteit Brussel' and the 'Universitair Ziekenhuis Brussel'.

Before starting the isolation, everything was disinfected as much as possible (working tools, working solutions and apparatus) and the fact that the samples should be on ice when possible was taken into account. The sample was transported from the hospital to the laboratory on ice (4°C) in a 50mL Falcon tube containing 25mL of sterile Hanks' Balanced Solution (HBSS) (Gibco by Life Technologies™). The content of the tube was poured into a 10 cm petridish and, with forceps and scissors, the maximum blood was removed by rubbing over the sample and the tissue was cut in small pieces of 3-5mm^2. With the epidermis sided up, each piece of the previous step was transferred to a new petridish with 25mL of sterile HBSS on it. The tissue was incubated at 4°C overnight for approximately 20h with 500µL of Liberase™ Research Grade solution (Roche Applied Science, Vilvoorde, Belgium) that was dripped over the samples with a 1mL micropipette. This solution will allow the dissociation of the epidermis because is a mixture of collagenase and neutral protease enzymes that have as targets the collagen and non-collagen proteins that comprise the intercellular matrix. After the incubation time the epidermis was removed, as well as the remaining blood vessels and adipose tissue. The samples were cut into smaller pieces (1-2mm^2), transferred to a 50mL Falcon tube along with the supernatant and incubated at 37°C for 20 min. On the last minute of incubation 400µL of DNase I (2mg/mL) (Sigma, Bornem, Belgium) were added to the tube to reduce the aggregation of cells. Afterwards, samples were incubated on ice (4°C) for 5 minutes with 10% of FBS (Perbio Science, Hyclone, Erembodegem, Belgium) to inactivate all enzymes and then were shortly centrifuged at 1200 rpm to get down the larger pieces. The supernatant was next removed and only 2mL were left to maintain the pellet submerged.

A mechanical dissociation was done by grinding the samples for 2 min with a 10mL pipette and, after that, 8mL of hSKP wash medium were added to the tube that was then centrifuged 10s at 1200 rpm. The supernatant was collected and filtered through a 70µm filter at 4°C. This process was repeated until 50mL of filtered supernatant was obtained or until there was no more tissue left over. Upon the dissociation step, the collected supernatant was centrifuged for 6

minutes at 1200 rpm and the obtained pellet was re-suspended with 1mL of hSKP wash medium.

Upon the isolation procedure, viable cells were counted in a TC10^{TM} automated cell counter (Bio-Rad® by Life Science) by adding 10µL of Trypan Blue dye (Bio-Rad®) to 10µL of the obtained cell suspension. Typically yield for one tissue sample is between 5 and 15×10^6 viable cells depending on the tissue size and origin. A cell density of 20 000 cells/cm^2 (1.5×10^6 cells per T75 flask) was applied for culturing in suspension. For a T75 flask 24mL of previously warmed up hSKP wash medium and 6mL of B27 Supplement (Life Technologies) were used. The cells were homogenized by cross agitation, incubated at 37°C and 5% CO_2 and the growth media was refreshed every 2-3 days through the addition of 2mL of B27. Typically multipotent spheres are formed from day 5-7 on like floating colonies. [48][49]

3.3. Dissociation of human skin-derived stem cells spheres

After 2 weeks, hSKP formed three-dimensional spheres that needed to be split and plated as a monolayer cell culture. The spheres were then centrifuged at 1200 rpm for 4 minutes and next digested with 2mL of Tryple Solution (Tryple^{TM} Express Enzyme, by Life Technologies) at 37°C for 12 minutes. After this digestion period, the Tryple Solution was inactivated by the addition of 20mL of hSKP wash medium and the cells were centrifuged one more time to obtain a pellet. The newly dissociated cells were re-suspended in 1mL of culture medium, counted and seeded at a density of 1.3x 10^4 cells/cm^2 for further culture as monolayers. Each T75 culture flask contained hSKP wash medium enriched with 20% of B27 Supplement and 5% of FBS that facilitates the cells attachment to the flask. The medium was refreshed on the following day so that the FBS could be removed and on every 2-3 days after that. Hereafter, the cells could be cultured in monolayers or frozen as described above.

3.4. Hepatic differentiation of human skin-derived stem cells

hSKP between 3 and 7 passages were cultivated at 90% confluency and seeded on collagen type 1 (BD Biosciences)-coated 24-well plates or T75 culture flasks (both BD Falcon) in hSKP basal medium (whose composition has already been previously mentioned). The concentration of the collagen working solution was 0.1mg/mL in 0.02M acetic acid solution. Hepatic differentiation of hSKP was started when the cells reached 90% cell confluence and was carried out using a 24-day protocol in which the cells were exposed in a time-dependent manner to hepatogenic factors (growth factors and cytokines) such as: Activin A (Life Technologies), fibroblast growth factor 4 (FGF4) (Life Technologies), bone morphogenetic protein 4 (BMP4) (Life Technologies), hepatocyte growth factor (HGF) (Life Technologies), insulin-transferin-sodium selenite solution (ITS) (Sigma-Aldrich), dexamethasone (DEX) (Sigma-Aldrich) and oncostatin M (OSM) (Life Technologies). The obtained differentiated hepatocyte-like cells are further referred to as hepatic progenitor cells obtained from human skin-derived precursors (hSKP-HPC). [50][49] The hSKP basal medium was changed and supplemented as the following table shows:

Table 3.1 **– hSKPs differentiation process.** Layout of the sequential hepatogenic differentiation protocol.

Day	Supplement	Concentrations		Volume (final volume of basal medium=50Ml)
		Stock	Final	
D0	Activin A	2.5µg/mL	50ng/mL	1000µL
D1	Activin A	2.5µg/mL	25ng/mL	500µL
	FGF4	2.5µg/mL	5ng/mL	100µL
	BMP4	1.0µg/mL	10ng/mL	500µL
D3	FGF4	2.5µg/mL	10ng/mL	200µL
	BMP4	1.0µg/mL	20ng/mL	1000µL
D6	FGF4	2.5µg/mL	5ng/mL	100µL
	BMP4	1.0µg/mL	10ng/mL	500µL
	HGF	2.0µg/mL	30ng/mL	750µL
	ITS	1.0 (v/v)	0.5% (v/v)	250µL
D9	HGF	2.0µg/mL	30ng/mL	750µL
	ITS	1.0% (v/v)	0.25% (v/v)	125µL
	DEX	100µg/mL	0.02ng/mL	10µL
D12	HGF	2.0µg/mL	20ng/mL	500µL
	DEX	100µg/mL	0.02ng/mL	10µL
D15 to D24 (every 3 days)	HGF	2.0µg/mL	20ng/mL	500µL
	DEX	100µg/mL	0.02ng/mL	10µL
	OSM	1.0µg/mL	10ng/mL	500µL

3.5. Cell Viability Assay

The reduction of tetrazolium salts is widely accepted as a reliable way to examine cell population's response to external factors. 2-EH cytotoxicity in HepG2 cells was determined by the 3-(4,5-dimethylthiazol-2-yl)-2,5-diphenyltetrazolium bromide (MTT) viability assay that measures the cell proliferation rate and conversely, when metabolic events lead to apoptosis or necrosis, the reduction in cell viability. The yellow MTT is reduced into formazan by metabolically active cells, in part by the action of dehydrogenase enzymes, to use reducing equivalents donated by NADH or NADPH (*Figure 3.1*). On the other hand, dead cells lost their mitochondrial activity and don´t have the ability to convert MTT into formazan. The resulting intracellular purple formazan is directly proportional to the number of viable cells and the precipitate must be solubilized prior to recording absorbance readings. This product has an absorbance maximum near 570nm and can be quantified by a plate reading spectrophotometer. [51]

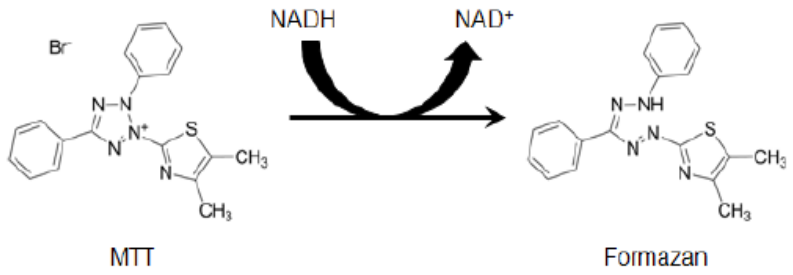

Figure 3.1 – **MTT reaction**. Structures of MTT and coloured formazan product.

The HepG2 cells were exposed for 24 hours to 2-EH concentrations ranging from 0.05mM to 5mM (C1) and the test was conducted in triplicate in a 96 microwell plate with the following layout (*Figure 3.2*).

The MTT solutions must be prepared *ex tempore* and should be protected from light. Two solutions were prepared, stock solution (10×, 5mg/ml) with PBS and working solution (1×, 0.5mg/ml) with medium. After the incubation period with 2-EH, the cells were washed with PBS and 250µL of pre-heated MTT working solution was added to all wells. The plate was incubated for 2.5h at 37°C, 5%CO_2, once again the cells were washed with PBS and the resulting precipitate was dissolved with DMSO (100µl per well). After a 4 minutes period at 100 rpm on a microtiter plate shaker, the abortion of the resulting coloured solution was measured at 570nm in a spectrophotometer, using the blanks as a reference.

A sub-cytotoxic concentration was determined by 4 parameter logistic nonlinear regression analysis of the obtained dose response curves. This analysis was performed with Masterplex Readerfit 2010 software (Hitashi Solutions, USA).

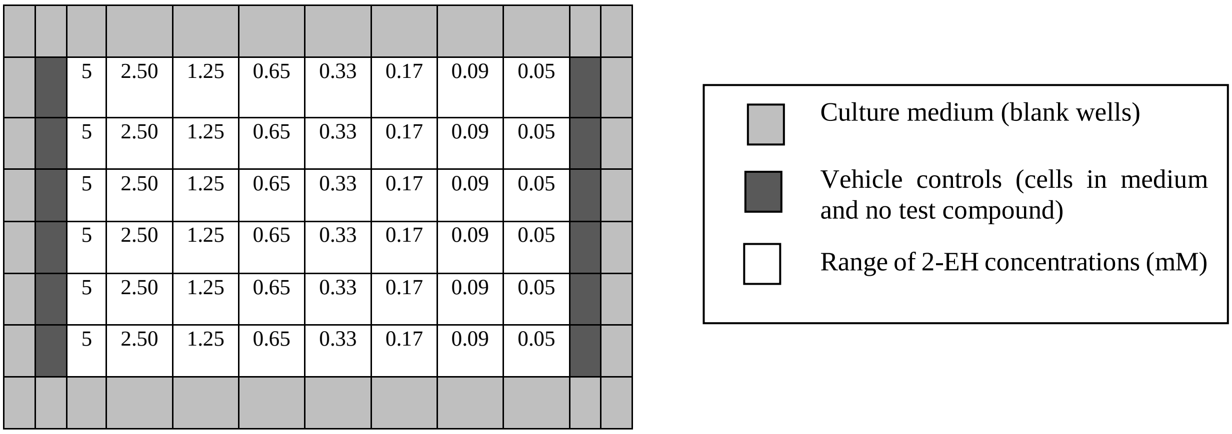

Figure 3.2 **- Cell viability assay layout.**

3.6. Cells exposure to steatogenic compounds

The different cell lines were exposed to several compounds such as Na-OA, Tetracycline, Na-VPA and 2-EH and to the corresponding control solutions. For cytochemical staining, the exposure time was 72h and for RNA extraction was 24h.

The concentrations of the compounds were used according to its inhibitory concentration (IC) found in literature or in previous experiments. [52] The IC_{10} reflects the reduction 10% of cell viability.

All further experiments, with both differentiated and undifferentiated hSKPs were based on the same donor to rule out donor variability.

Table 3.2 **- Cells exposure to steatogenic compounds.** Concentrations and dilutions used to expose the several compounds and controls to the different cell lines.

Cell line	Compounds	Concentration (mM)	Dilutions
HepG2	Na-OA	1	3.0mg Na-OA + 0.5mL **FBS** (hSKP) + 9.5mL HepG2 culture medium
	Tetra	0.52	50 mg Tet + 1mL **DMSO** → stock solution 104mM Dilute 200x: 50µl stock + 10mL culture medium
	Na VPA	0.5	3.6mg Na-VPA + 5mL culture **medium** → stock solution 5mM Dilute 100x: 100µl stock + 10mL culture medium
	2-EH	1.25	171uL 2-EH + 1mL **DMSO** → stock solution 1.1M Dilute 200x: 11.36µL in 10mL HepG2 culture medium
	Control 1 Na-OA	-	9.5mL HepG2 culture medium + 0.5mLFBS (hSKP)
	Control 2 Tetra, 2-EH	-	50µL DMSO + 10mL HepG2 culture medium
	Control 3 Na-VPA	-	10mL culture medium
hSKPs HPC	Na-OA	0.07	1.98mg + 2mL FBS → stock solution 3.5mM Dilute 50x: 400µl stock + 100µL DMSO + 19.5mL culture medium
	Tet	0.56	25mg Tet + 0.5mL DMSO → stock solution 112mM Dilute 200x: 100µl stock + 19.9mL culture medium
	2-EH	2.08	65uL 2-EH + 1mL DMSO → stock solution 416M Dilute 200x: 100uL in 19.9mL culture medium
	Control 1	-	100µL DMSO + 20mL culture medium
Undifferentiated hSKPs	Na-OA	0.07	1,98mg + 2mL FBS → stock solution 3.5mM Dilute 50x: 300µl stock + 14.7mL culture medium
	Tet	0.56	25 mg Tet + 0.5mL DMSO → stock solution 112mM Dilute 200x: 75µl stock + 14.9mL culture medium
	2-EH	2.08	65uL 2-EH + 1mL DMSO → stock solution 416 M Dilute 200x: 75uL stock in 14.9mL culture medium
	Control 1		75µL DMSO + 14.9mL culture medium

For RNA extraction, all experiments with HepG2 and hSKPs were performed in triplicate leading to three different samples per one 24 microwell plate. When working with HepG2, one extra compound was tested (Na-VPA) and 3 different controls were used. On the account of practical issues, only one control was used when working with hSKPs as shown in the previous table A.

Na-OA 1	Na-OA 1	Na-OA 2	Na-OA 2	Na-OA 3	Na-OA 3
Na-OA 1	Na-OA 1	Na-OA 2	Na-OA 2	Na-OA 3	Na-OA 3
Na-OA 1	Na-OA 1	Na-OA 2	Na-OA 2	Na-OA 3	Na-OA 3
Na-OA 1	Na-OA 1	Na-OA 2	Na-OA 2	Na-OA 3	Na-OA 3

Tetra 1	Tetra 1	Tetra 2	Tetra 2	Tetra 3	Tetra 3
Tetra 1	Tetra 1	Tetra 2	Tetra 2	Tetra 3	Tetra 3
Tetra 1	Tetra 1	Tetra 2	Tetra 2	Tetra 3	Tetra 3
Tetra 1	Tetra 1	Tetra 2	Tetra 2	Tetra 3	Tetra 3

2-EH 1	2-EH 1	2-EH 2	2-EH 2	2-EH 3	2-EH 3
2-EH 1	2-EH 1	2-EH 2	2-EH 2	2-EH 3	2-EH 3
2-EH 1	2-EH 1	2-EH 2	2-EH 2	2-EH 3	2-EH 3
2-EH 1	2-EH 1	2-EH 2	2-EH 2	2-EH 3	2-EH 3

Na-VPA 1	Na-VPA 1	Na-VPA 2	Na-VPA 2	Na-VPA 3	Na-VPA 3
Na-VPA 1	Na-VPA 1	Na-VPA 2	Na-VPA 2	Na-VPA 3	Na-VPA 3
Na-VPA 1	Na-VPA 1	Na-VPA 2	Na-VPA 2	Na-VPA 3	Na-VPA 3
Na-VPA 1	Na-VPA 1	Na-VPA 2	Na-VPA 2	Na-VPA 3	Na-VPA 3

CTL3 1	CTL3 1	CTL3 2	CTL3 2	CTL3 3	CTL3 3
CTL3 1	CTL3 1	CTL3 2	CTL3 2	CTL3 3	CTL3 3
CTL3 1	CTL3 1	CTL3 2	CTL3 2	CTL3 3	CTL3 3
CTL3 1	CTL3 1	CTL3 2	CTL3 2	CTL3 3	CTL3 3

CTL1 1	CTL1 1	CTL1 2	CTL1 2	CTL1 3	CTL1 3
CTL1 1	CTL1 1	CTL1 2	CTL1 2	CTL1 3	CTL1 3
CTL1 1	CTL1 1	CTL1 2	CTL1 2	CTL1 3	CTL1 3
CTL1 1	CTL1 1	CTL1 2	CTL1 2	CTL1 3	CTL1 3

CTL2 1	CTL2 1	CTL2 2	CTL2 2	CTL2 3	CTL2 3
CTL2 1	CTL2 1	CTL2 2	CTL2 2	CTL2 3	CTL2 3
CTL2 1	CTL2 1	CTL2 2	CTL2 2	CTL2 3	CTL2 3
CTL2 1	CTL2 1	CTL2 2	CTL2 2	CTL2 3	CTL2 3

CTL 1	CTL 1	CTL 2	CTL 2	CTL 3	CTL 3
CTL 1	CTL 1	CTL 2	CTL 2	CTL 3	CTL 3
CTL 1	CTL 1	CTL 2	CTL 2	CTL 3	CTL 3
CTL 1	CTL 1	CTL 2	CTL 2	CTL 3	CTL 3

Figure 3.3 – **Exposure layouts for RNA extraction.** 24 microwell plate layouts that were used to expose the HepG2 and hSKP cells to the steatogenic compounds and do the RNA extraction.

	Na-AO	Na-AO	CTL	CTL	
	Tetra	Tetra	CTL	CTL	
	2-EH	2-EH	CTL	CTL	
	Na-VPA	Na-VPA			

Figure 3.4 **- Exposure layouts for staining.** 24 microwell plate layouts that were used to expose the HepG2 and hSKP cells to the steatogenic compounds and do the cytochemical staining. At least 2 wells were used per condition.

3.7. Cytochemical Staining (LipidTOX)

The LipidTOX™ neutral lipid stain has an extremely high affinity for neutral lipid droplets and can be detected by fluorescence microscopy (fluorescence excitation/emission maxima: 495/505 nm). The addition of this probe to the exposed cells will allow the analysis of the intracellular accumulation of lipids, known as steatosis, induced by the steatogenic compounds. These reagent is added to formaldehyde-fixed cells seeded in 24 microwell plates.

After 72h of incubation, the exposure medium was removed and the cells were washed with PBS, fixed with 4% paraformaldehyde fixate solution and washed with PBS one more time. The cells in each well were incubated for 15 minutes with 0,5mL of 0,1% of LipidTOX™ green solution. After that, the LipidTOX™ was removed, the cells were washed with PBS and 1 drop Vectashield® Mounting Medium containing DAPI was added on each well. The samples were observed with fluorescence microscope.

3.8. RNA extraction

Total RNA was extracted from all samples using the GenElute^{TM} Mammalian Total RNA Purification Miniprep Kit (Sigma-Aldrich). After exposure to the steatogenic compounds for 24 hours, the exposed cells and respective controls were harvested in RNAse free 1,5mL tubes. Firstly, the media was removed and then the RNA was extracted from the multi-well plates with 500µL of Lysis Solution with 1% of 2-mercaptoethanol per exposure (8 or 12 wells depending on the type of cells in study). The 2-mercaptoethanol is a reducing agent that will irreversibly denature intracellular RNases that are released during the lysis step thus avoiding RNA degradation. After the harvesting, the lysates were transferred to blue filtration columns and shortly spin to remove cellular debris and shears DNA. 500µL of 70% ethanol were added to the filtered lysate in each tube to prepare the samples for binding. After pipetting thoroughly to mix, the lysate/ethanol mixtures were transferred to new collection tubes in 2 steps (500µL each time), centrifuged, the flow-through liquid was discard and the collection tube retained. Afterwards, the column was washed with 250µL wash solution 1 and, to avoid DNA contamination, each preparation was incubated for 1 minute with a mix of 10µL of DNase I with 70µL of DNase Digest Buffer. After the incubation period, 250µL of wash solution were

added, the tubes were shortly centrifuged and the binding columns into a fresh 2.0mL collection tube. Two additional wash steps were done with 2×500µL of wash solution 2. The binding column was transferred to a fresh 2mL collection tube, 50µL of the Elution Solution were pipetted into the binding column that was then centrifuged at maximum speed for 1 minute. Isolated and purified RNA was now in the flow-through eluate and acid nucleic purity and quantity were determined by spectrophotometric analysis using a Nanodrop spectrophotometer (Thermo Scientific). The measurements were performed using 2µL of each sample and 2µL of the elution solution that was used as blank, at a wavelength of 260nm.

3.9. cDNA preparation and Clean-up

After total RNA isolation, mRNA was reverse-transcribed into cDNA using an iScript-cDNA Synthesis Kit (BioRad), followed by cDNA purification with a GenElute PCR Clean-Up Kit (Sigma-Aldrich). This step will generate complementary single-stranded DNA (cDNA) from each mRNA template.

According to the obtained RNA concentrations, the necessary amount of each sample (µL) to have 0.5µg of RNA was calculated and then diluted in the correct amount of diethylpyrocarbonate-treated water (DPEC), that will inactivate RNase enzymes, to perform a final volume of 30µL. 8µL of 5x iScript Reaction Mix, which contained oligo(dT) and random hexamer primers, and 2µL of iScript Reverse Transcriptase were added to each sample. For each sample, two series of 0.5µg of RNA were made and brought together on the last step of the clean-up. The 200µL vials were shortly vortexed and placed in the 96-well BioRad C1000 Termal Cycler to incubate. After a sequence of several thermal cycles (5 minutes at 5°C, 30 minutes at 42°C and 5 minutes at 85°C) the cDNA samples were purified from other components in the reactions, such as excess primers, nucleotides, DNA polymerase, oil and salts using the GenElute™ PCR Clean-Up Kit (Sigma-Aldrich). DNA was bound on a silica membrane within the spin column and previously washed, cleaned and eluted with the elution solution. The cDNA samples were stored at -80°C until being used in gene expression studies.

3.10. Quantitative Polymerase Chain Reaction

Polymerase chain reaction (PCR) is a technique used to exponentially amplify a specific target DNA or cDNA template sequence, allowing for the gene expression analysis. In quantitative PCR (qPCR), the accumulation of amplification product is measured as the reaction progresses, in real time, with product quantification after each cycle. Reactions are generally run for 40 cycles and each cycle is composed of several steps such as incubation of the cDNA, denaturation of the double-stranded DNA, annealing of the primers to specific sequences of DNA and extension by the addition of dNTPs (deoxynucleotide triphosphates) by the DNA polymerase. As the DNA polymerase loses activity or the dNTPs and primers are consumed, the reaction rate reaches a plateau.

In order to detect the increasing amount of DNA, the qPCR products are fluorescently labelled using fluorogenic probes that are target specific oligonucleotides and produce a fluorescent signal only when the target DNA is amplified during qPCR. The measured fluorescence is proportional to the total amount of amplicon and is measured by an instrument that combines thermal cycling with fluorescent dye scanning capability. By plotting fluorescence against the cycle number, the real-time PCR instrument generates an amplification plot that represents the accumulation of product over the duration of the entire PCR reaction. [53][54]

The cDNA products were quantitatively amplified using TaqMan® Gene Expression Assays (Life Technologies) and primers specific to the target genes of interest. As already mentioned, the following genes were evaluated: *ACADSB, APOB, CD36, CPT1A, FASN* and *SCD1*. To normalize the qPCR data, several stable reference genes were used: 18S ribosomal RNA (*18S*), actin beta (*ACTB*), beta-2-microglobulin (*B2M*), glyceraldehyde 3-phosphate dehydrogenase (*GAPDH*), hydroxy-methylbilane synthase (*HMBS*) and ubiquitin C (*UBC*). All samples were tested in duplicate, and each run included a negative control (non-template control, NTC) and a serial dilution of a pooled cDNA mix from all cDNA samples to estimate the qPCR efficiency.

The qPCR reaction mix consisted of 10µL TaqMan Fast Advanced Master Mix (Life Technologies), 1µL 20× Assay-on-Demand Mix (Life Technologies), and 2mL of cDNA in a 20µL volume adjusted with DNase-/ RNase-free water. TaqMan Fast Advanced Master Mix is supplied at a 2X concentration and contains AmpliTaq® Fast DNA Polymerase, uracil-N glycosylase (UNG), dNTPs with dUTP, ROX™ dye (passive reference), and optimized buffer components.

qPCR conditions, using a StepOne Plus system (Life Technologies) were as follows: incubation for 20 s at 95°C, followed by 40 cycles of 1s denaturation at 95°C, and annealing for 20s at 60°C (Life Technologies). Results are expressed as the fold changes normalized against the geometric means of reference genes using Qbase PLUS software (Biogazelle). Statistical analyses were performed by an unpaired t-test.

The fold changes in gene expression were obtained by the calculation of the $\Delta\Delta C_T$, a comparative method that provides a relative quantification. This method is based in a threshold which is an arbitrary level of fluorescence within the linear phase at which all amplification plots are analysed. Then, the C_T that is the PCR cycle at which each amplification plot reaches this threshold, was determined. For each sample, the ΔC_T was calculated by normalizing the C_T of the gene of interest with the mean of the C_T of the housekeeping genes selected by the geNorm.

$$\Delta C_T(\text{sample}) = C_T(\text{gene of interest}) - C_T(\text{housekeeping genes}) \quad (1)$$

Posteriorly, the $\Delta\Delta C_T$ was calculated by normalizing each sample with the respective control sample.

$$\Delta\Delta C_T(\text{sample}) = \Delta C_T(\text{sample}) - \Delta C_T(\text{control}) \quad (2)$$

The resulting $\Delta\Delta C_T$ value is incorporated to determine the fold change in expression.

$$2^{-\Delta\Delta CT} \quad (3)$$

3.10.1. Layouts and standard lines

Reaction per well	
Taqman universal PCR master mix	10µL
Distilled water	7µL
Assay-on-demand mix	1µL
cDNA sample	2µL
	20µL

Standard serie (10 series):	
Standard 1	6µL × 21 samples = 126µL
Standard 1/5	25µL St1 + 100µL DEPC
Standard1/25	25µL St1/5 + 100µL DEPC
Standard 1/125	25µL St1/25 + 100µL DEPC
Standard 1/625	25µL St1/125 + 100µL DEPC

PCR: HepG2 + Na AO + Tet + Na VPA + 2 EH												21/03/2107
	1	2	3	4	5	6	7	8	9	10	11	12
A	Standard 1	Standard 1	Standard 1/5	Standard 1/5	Standard 1/25	Standard 1/25	Standard 1/125	Standard 1/125	Standard 1/622	Standard 1/625	Negative CTL	Negative CTL
B	Na-OA 1	Na-OA 1	Na-OA 2	Na-OA 2	Na-OA 3	Na-OA 3	CTL1 1	CTL1 1	CTL1 2	CTL1 2	CTL1 3	CTL1 3
C	Tet 1	Tet 1	Tet 2	Tet 2	Tet 3	Tet 3	CTL2 1	CTL2 1	CTL2 2	CTL2 2	CTL2 3	CTL2 3
D	Na-VPA 1	Na-VPA 1	Na-VPA 2	Na-VPA 2	Na-VPA 3	Na-VPA 3	CTL3 1	CTL3 1	CTL3 2	CTL3 2	CTL3 3	CTL3 3
E	2-EH 1	2-EH 1	2-EH 2	2-EH 2	2-EH 3	2-EH 3						
F												
G												
H												

CTL - Control

Plate 1	*18S*: Hs99999901_s1
Plate 2	*GAPDH*: Hs99999905_m1
Plate 3	*ACADSB*: Hs00155631_m1
Plate 4	*FASN*: Hs01005622_m1
Plate 5	*SCD1*: Hs01682761_m1
Plate 6	*CD36*:Hs00354519_m1
Plate 7	*APOB*: Hs00181142_m1
Plate 8	*CPT1A*: Hs00912671_m1
Plate 9	*B2M*: Hs99999907_m1
Plate 10	*HMBS*: Hs00609296_g1
Plate 11	*ACTB*: Hs99999903_m1

***Figure* 3.5 – HepG2 qPCR layout**. Reaction and composition of each well, standard line calculations and composition of the eleven plates.

Reaction per well	
Taqman universal PCR master mix	10µL
Distilled water	7µL
Assay-on-demand mix	1µL
cDNA sample	2µL
	20µL

Standard serie (10 series):	
Std 1	6µL * 12 samples = 72µL
Std 1/5	15µL St1 + 60µL DEPC
Std 1/25	15µL St1/5 + 60µL DEPC
Std 1/125	15µL St1/25 + 60µL DEPC
Std 1/625	15µL St1/125 + 60µL DEPC

PCR: hSKP and hSKP-HPC + Na AO + Tet + 2 EH												
	1	2	3	4	5	6	7	8	9	10	11	12
A	Standard 1	Standard 1	Standard 1/5	Standard 1/5	Standard 1/25	Standard 1/25	Standard 1/125	Standard 1/125	Standard 1/622	Standard 1/625	Negative CTL	Negative CTL
B	Tet 1	Tet 1	Tet 2	Tet 2	Tet 3	Tet 3	2-EH 1	2-EH 1	2-EH 2	2-EH 2	2-EH 3	2-EH 3
C	Na-OA 1	Na-OA 1	Na-OA 2	Na-OA 2	Na-OA 3	Na-OA 3	CTL1 1	CTL1 1	CTL1 2	CTL1 2	CTL1 3	CTL1 3
D												
E	Std 1	Std 1	Std 1/5	Std 1/5	Std 1/25	Std 1/25	Std 1/125	Std 1/125	Std 1/625	Std 1/625	NTC	NTC
F	Tet 1	Tet 1	Tet 2	Tet 2	Tet 3	Tet 3	2-EH 1	2-EH 1	2-EH 2	2-EH 2	2-EH 3	2-EH 3
G	Na-OA 1	Na-OA 1	Na-OA 2	Na-OA 2	Na-OA 3	Na-OA 3	CTL1 1	CTL1 1	CTL1 2	CTL1 2	CTL1 3	CTL1 3
H												

CTL - Control

hSPKP-HPC plates

Plate 1	*18S*: Hs99999901_s1
	SCD1: Hs01682761_m1
Plate 2	*B2M*: Hs99999907_m1
	HMBS: Hs00609296_g1
Plate 3	*GAPDH*: Hs99999905_m1
	CPT1A: Hs00912671_m1
Plate 4	*FASN*: Hs01005622_m1
Plate 5	*CD36*:Hs00354519_m1
	APOB: Hs00181142_m1
Plate 6	*ACTB*: Hs99999903_m1
	ACADSB: Hs00155631_m1

Undifferentiated hSPKP plates

Plate 1	*18S*: Hs99999901_s1
	SCD1: Hs01682761_m1
Plate 2	*B2M*: Hs99999907_m1
	HMBS: Hs00609296_g1
Plate 3	*GAPDH*: Hs99999905_m1
	CPT1A: Hs00912671_m1
Plate 4	*FASN*: Hs01005622_m1
Plate 5	*CD36*:Hs00354519_m1
	APOB: Hs00181142_m1
Plate 6	*UBC*: Hs00824723_m1
	ACADSB: Hs00155631_m1

***Figure* 3.6 – hSKP and hSKP-HPC qPCR layout.** Reaction and composition of each well, standard line calculations and composition of the twelve plates.

3.10.2. Normalization of real-time qPCR – geNorm

Several variables need to be controlled for gene-expression analysis, such as the amount of starting material or differences between cells in overall transcriptional activity. To control these factors and normalize the mRNA fraction, internal control genes referred as housekeeping genes are used. However, to confirm the presumed stability of the expression of these housekeeping genes, proper validation to identify the most stably expressed control genes and to determine the minimum number of genes required to calculate a reliable normalization factor must be done.

Five housekeeping genes were used per each run and according to the geNorm software analysis, only the most suitable ones were used to do the normalization calculations. The validation of the control genes relies on the principle that the expression ratio of two ideal internal control genes is identical in all samples. An increased variation in this ratio will correspond to a decreasing expression stability. The internal control gene-stability measure **M** is the average pairwise variation of a particular gene with all other control genes which means that the genes with the lowest M values have the most stable expression. Therefore, the exclusion of the gene(s) with the highest M value(s) result in a combination of housekeeping genes that have the most stable expression. The normalization factor must be based on the expression of multiple housekeeping genes so that is recommended the use at least three most stable internal control genes and stepwise inclusion of more control genes until the gene has no significant contribution to the newly calculated normalization factor. The pairwise variation $\mathbf{V_{n/n+1}}$ (n=number of internal control genes in use) determines the possible need of including more genes for normalization and is calculated between two sequential normalization factors (NF_n and NF_{n+1}). A large variation means that the added gene has a significant effect and should be included for the calculations of the normalization factor. Also, the considered cut-off value is 0.15, below which the additional control gene is not required.

[55]

4. Results

4.1. Characterization of the human hepatic cell systems

As previously mentioned, three different human hepatic cell systems were used in this study: HepG2, undifferentiated hSKP and hSKP-HPC cells. All the models were characterized when in culture and before starting any kind of experiences. This characterization was mainly done by observation of the cells by light microscopy.

4.1.1. HepG2

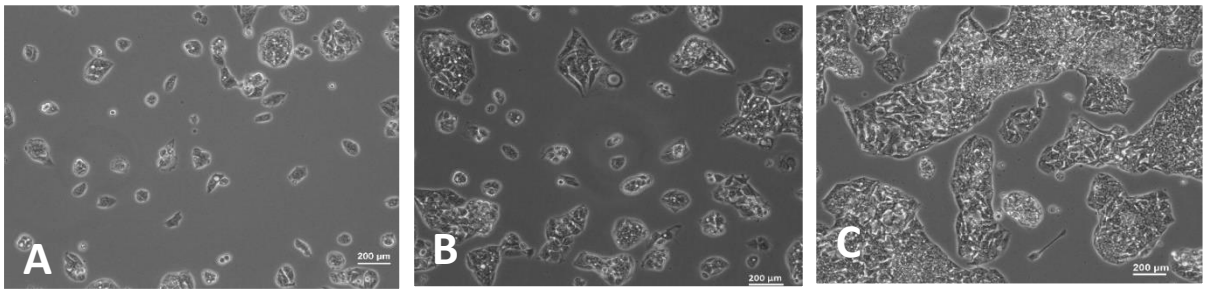

***Figure 4.1* – HepG2 cell line.** HepG2 cells in culture 1, 3 and 6 days after thaw (A, B, C respectively). The pictures were obtained by phase contrast microscopy with the 10× objective.

The hepatoma cells were flattened, grossly polygonal, and mainly arranged in monolayers with an epithelial morphology growing in small aggregates. In *Figure C*, the HepG2 at a high degree of confluency, are ready to be sub-cultured.

4.1.2. hSKPs

After the 2-day isolation procedure, hSKPs grown in suspension in T75 flasks with wash medium enriched with B27. Several contaminating cells, adherents to the culture flask, started to grow which led to the transfer of the medium to a new flask. The first hSKP multipotent floating spheres appeared in suspension 12 days after isolation *(Figure 4.2)* and were immediately transferred to new flasks.

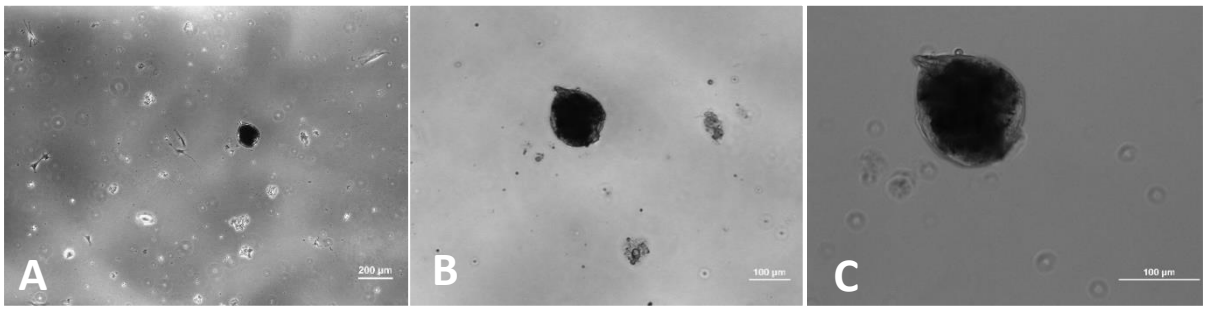

***Figure 4.2* - hSKP spheres**. hSKP spheres appeared 12 days after isolation and grown as spherical colonies in 3D expansion. In addition, several contaminating cells grown attached to the flask, as perceived in the pictures. The pictures were obtained by phase contrast microscopy with the 5×, 10× and 20× objective (A, B, C respectively).

After two weeks in culture, hSKP spheres were dissociated and plated as a monolayer cell culture in T75 culture flasks with a typical fibroblast-like appearance *(Figure 4.3).*

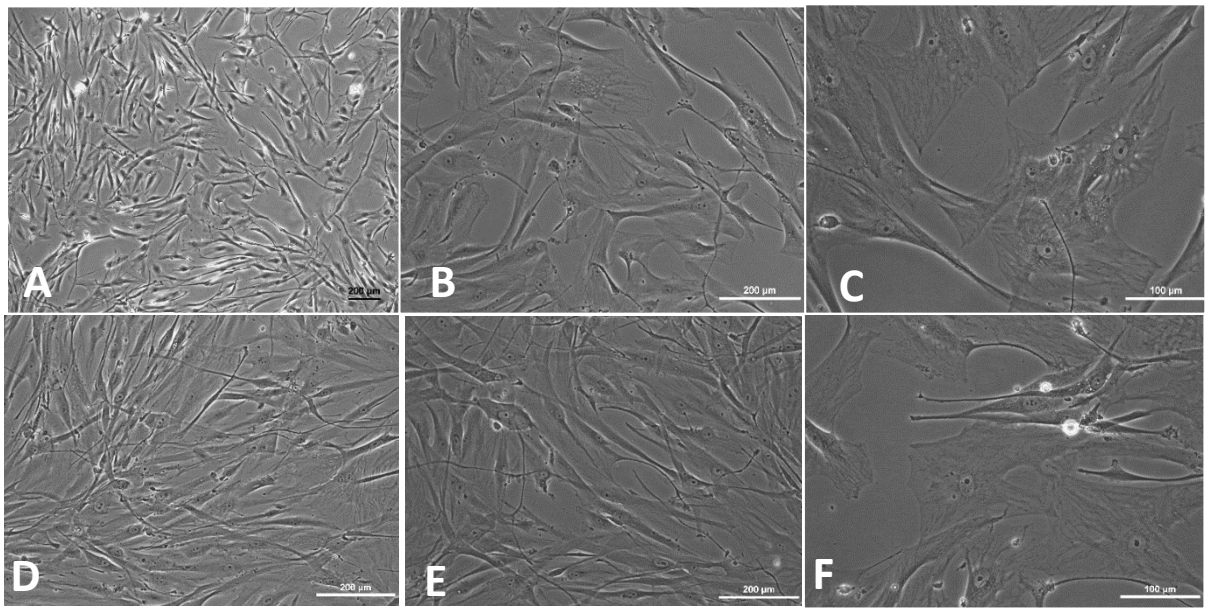

***Figure 4.3* – Undifferentiated hSKP.** Undifferentiated hSKP in monolayer 1 (A, B, C) and 4 days (D, E, F) after thaw. The pictures were obtained by phase contrast microscopy with the 5× (A, D), 10× (B, E) and 20× (C,F) objective.

When the hSKPs reached 90% confluency, the differentiation protocol was initiated and the cells were seeded on collagen type 1-coated 24-wells plates. Hepatic differentiation protocol lasted 24 days and resulted in a gradual morphological change of the cells accompanied with cell death. *(Figure 4.4)* As such, hSKP adopted a more polygonal-to-cuboidal cell shape with an epithelial-like structure. The cells increased in size and the nucleus become elongated.

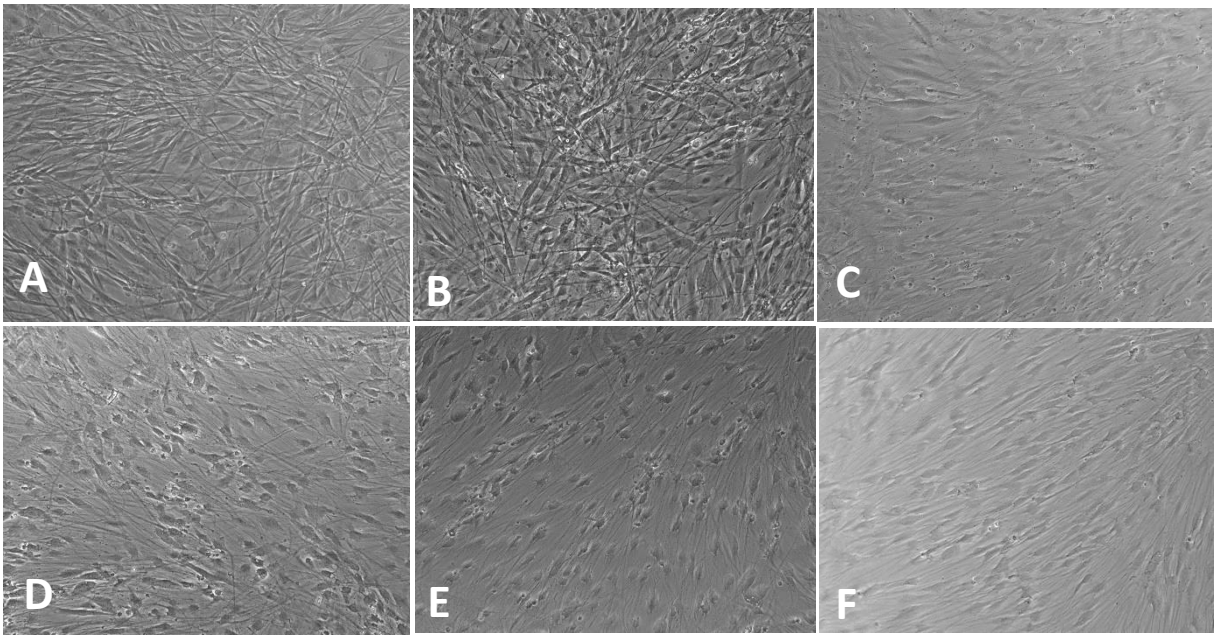

Figure 4.4 – hSKPs hepatic differentiation process. During the hSKPs hepatic differentiation process, the cells were exposed in a time-dependent manner to hepatogenic factors such as growth factors and cytokines, mimicking the liver embryogenesis *in vivo*. The pictures were taken in several different points of cell differentiation such as day 1 (A), day 3 (B), day 7 (C), day 13 (D), day 15 (E) and day 24 (F). The pictures were obtained by phase contrast microscopy with the 10× objective. Adapted from *Costa, Daniela O., 2016.* [52]

4.2. Determination of sub-cytotoxic dose of 2-ehtylhexanol

The maximum soluble concentrations of each compound used in the experiments in this thesis, were based on published data or obtained in previous experiments performed by the group. This allowed the determination of the IC_{10} (inhibitory concentration) values that reflect the reduction of cell viability by 10%. The IC_{10} of 2-ethylhexanol (2-EH) was determined by Costa, Daniela O. in 2016 and is 5.48 mM. [52]

However, when exposing HepG2 cells to this IC_{10} of 2-EH, a big percentage of dead cells was observed. For that reason, the cell viability assay was repeated to evaluate the range of concentrations that must be employed. *(Figure 4.5)*

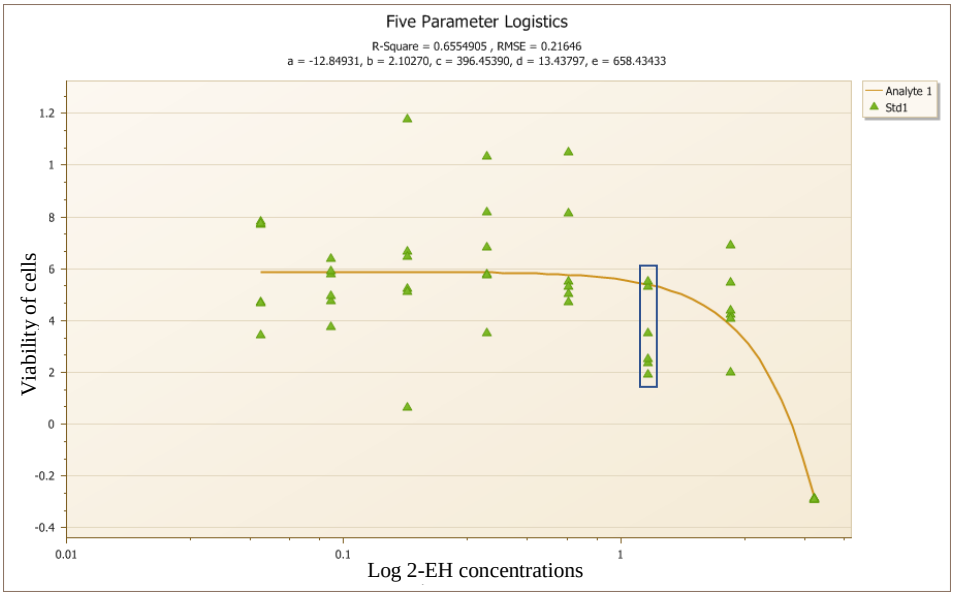

***Figure 4.5* – HepG2 viability assay after treatment with 2-EH.** Cell viability assay was determined by MTT assay after incubation of HepG2 with increasing concentrations of 2-EH (5; 2.50; 1.25; 0.65; 0.33; 0.17; 0.09; 0.05mM).

When analysing the graphic, it is clear that within the same 2-EH concentration the viability of cells is variable. This might be due to poor dissolution of the compound. To obtain fully reliable results the assay should be repeated, however, this could not be done during Erasmus exchange period.

Nevertheless, a sub cytotoxic concentration, namely 1.25mM, was determined and could be used in the following experiments.

4.3. Cytochemical Staining

After the 72h incubation period, the intracellular accumulation of lipids was evaluated at a phenotypic level in each *in vitro* model. On the one hand, the LipidTOX^{TM} probe has affinity for neutral lipid droplets and on the other hand, DAPI will colour nuclei, securing the identification of the fixed cells. Therefore, when examining with fluorescence microscopy, lipids droplets will be green and the cell nucleus blue.

In order to analyse correctly the pictures, each figure includes a phase contrast image, a DAPI coloured image, and a LipidTOX^{TM} green image. A merged image combines the two fluoresce images and allows the clear observation of lipid accumulation. Although most pictures will present a green background, lipid accumulation is only considered when green dots are present in the images.

Due to practical issues, in this study it was not possible to obtain photos of cytochemical staining of hSKP-HPC. The presented photos were adapted from *Costa, Daniela O., 2016.* [52] whose applied methods and concentrations were exactly as described above in material and methods chapter.

4.3.1. Sodium Oleate (Na-OA)

The three hepatic cell models were incubated with Na-OA for 72h with the corresponding IC_{10} determined in previous studies. The Na-OA sub-cytotoxic concentrations used were 1mM for HepG2 and 0.07mM for hSKPs and hSKPs HPC.

The HepG2 treatment *(Figure 4.6 B)* showed accumulation of TGs, organized in lipid droplets. However, the HepG2 control *(Figure 4.6 A)* also exhibited some lipid accumulation.

When it comes to undifferentiated hSKPs and hSKP-HPC, the lipids deposition is much more distinguishable in the treatment with Na-OA *(Figure 4.7 B* and *4.8 B)* than in the control *(Figure 4.7 A and 4.8 A)*, suggesting that Na-OA induces steatosis in hSKPs.

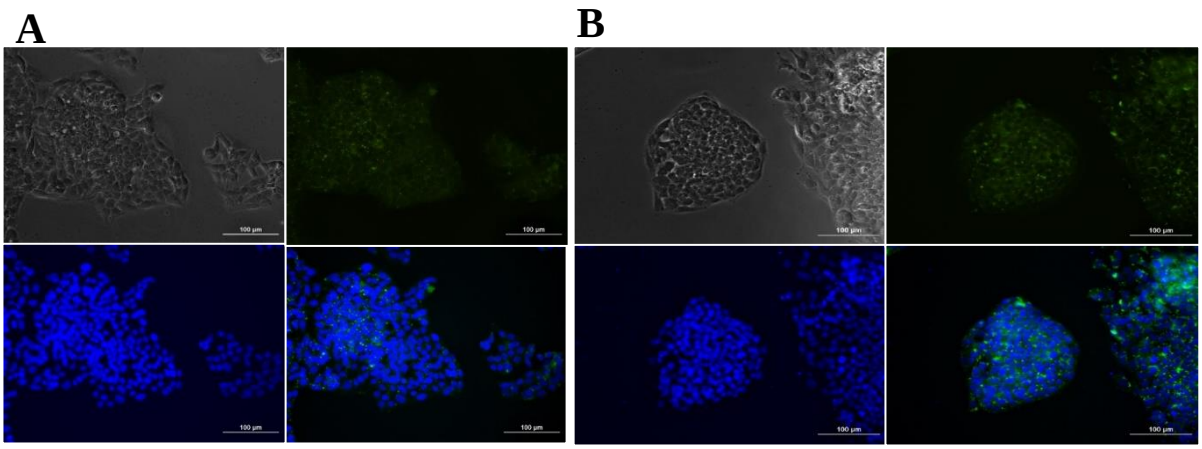

***Figure 4.6* – HepG2 treatment with sodium oleate.** HepG2 cytochemical neutral lipid staining after treatment with medium and FBS (control) **(A)** and 1mM Na-OA **(B).** The pictures were obtained by fluorescence microscope with the 20× objective

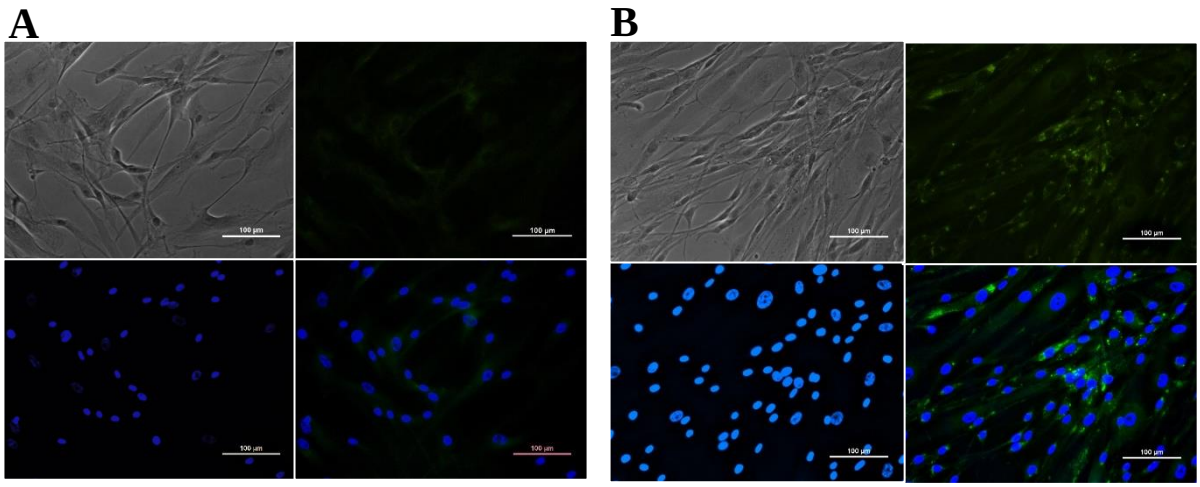

***Figure 4.7* - hSKPs treatment with sodium oleate.** Undifferentiated hSKPs cytochemical neutral lipid staining after treatment with DMSO and FBS (control) **(A)** and 0.07mM Na-OA **(B).** The pictures were obtained by fluorescence microscope with the 20× objective.

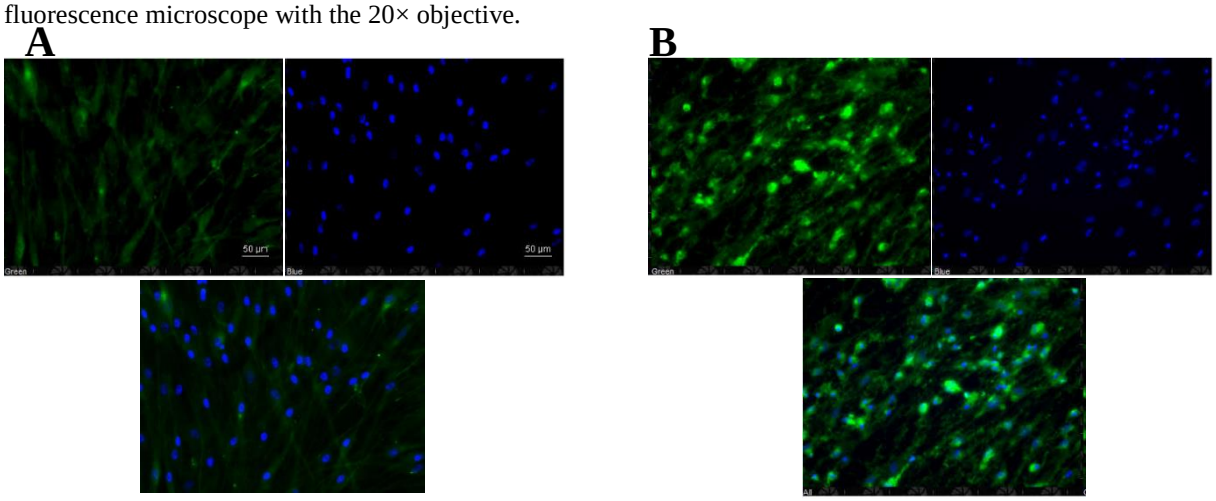

***Figure 4.8* – hSKP-HPC treatment with sodium oleate.** Differentiated hSKPs cytochemical neutral lipid staining after treatment with DMSO and FBS (control) **(A)** and 0.07mM Na-OA **(B).** The pictures were obtained by fluorescence microscope with the 20× objective. Adapted from *Costa, Daniela O., 2016.* [52]

.

4.3.2. Tetracycline (Tet)

The same approach was used to determinate the capacity of tetracycline to induce steatosis. The Tet sub-cytotoxic concentrations used were 0.52mM with HepG2 and 0.56mM with hSKPs and hSKPs HPC.

HepG2 exposed to Tet *(Figure 4.9 B)* showed accumulation of lipid droplets and also morphological changes. Comparing with the control *(Figure 4.9 A)*, the cells exposed to Tet are elongated and do not form well defined clusters. However, the lipid accumulation after Tet exposure is not that significant.

The undifferentiated hSKPs exposure to Tet showed slight green dotted clusters *(Figure 4.10 B)* representing the lipid accumulation induced by this drug. A much higher degree of the same green dotted areas was present in hSKP-HPC exposed to Tet. *(Figure 4.11 B)*

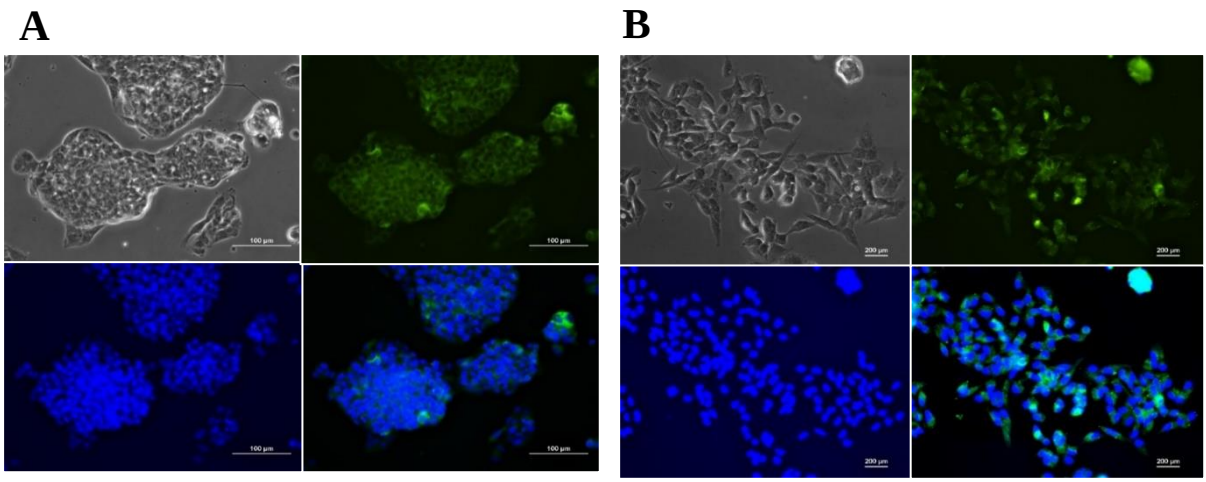

Figure 4.9 **- HepG2 treatment with tetracycline.** HepG2 cytochemical neutral lipid staining after treatment with medium and DMSO (control) **(A)** and 0,52mM Tet **(B).** The pictures were obtained by fluorescence microscope with the 20× objective.

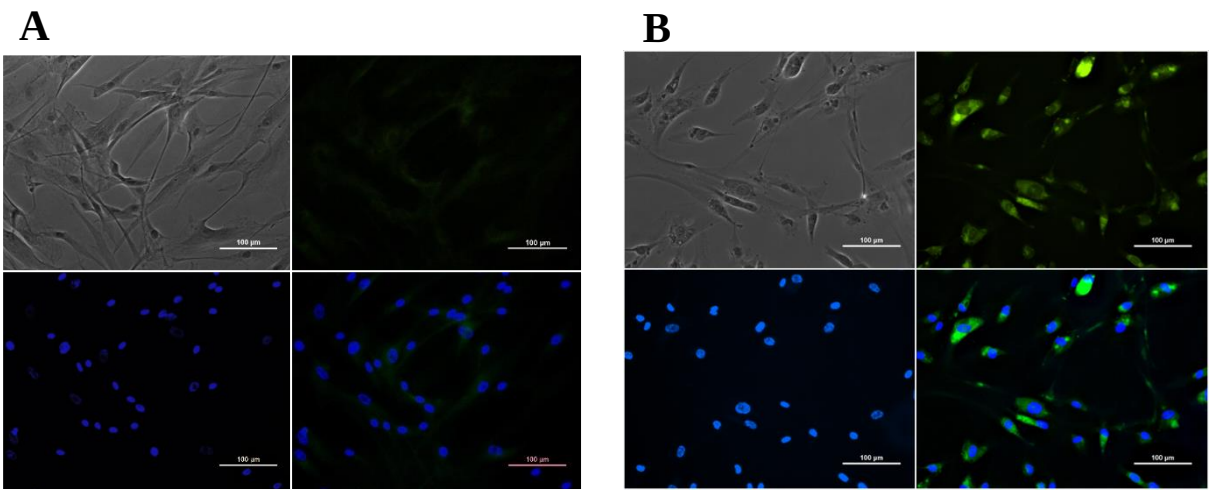

Figure 4.10 **- hSKPs treatment with tetracycline.** Undifferentiated hSKPs cytochemical neutral lipid staining after treatment with DMSO and FBS (control) **(A)** and 0,56 mM Tet **(B).** The pictures were obtained by fluorescence microscope with the 20× objective.

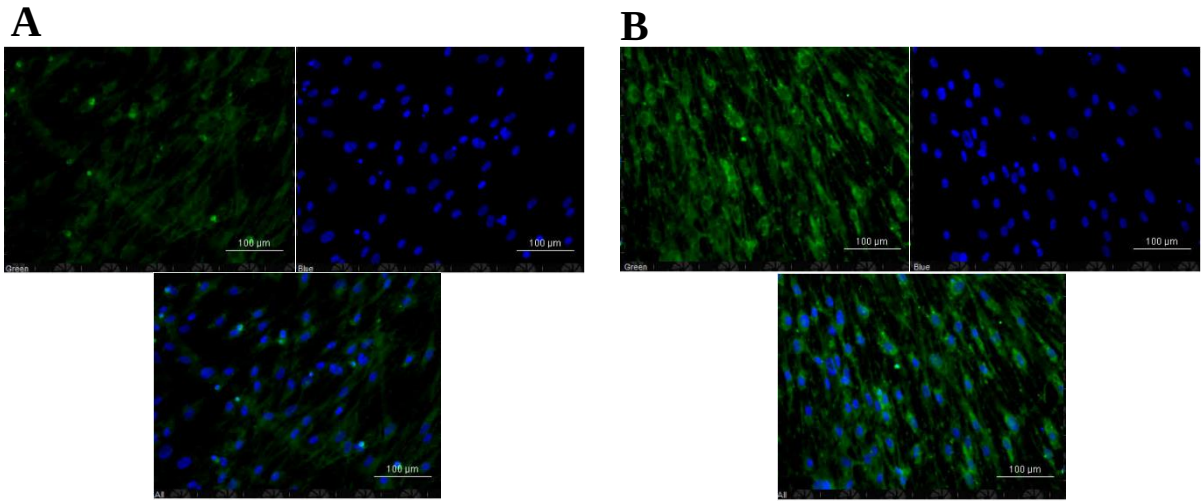

Figure 4.11 **– hSKP-HPC treatment with tetracycline.** Differentiated hSKPs cytochemical neutral lipid staining after treatment with DMSO and FBS (control) **(A)** and 0,56 mM Tet **(B).** The pictures were obtained by fluorescence microscope with the 20× objective. Adapted from *Costa, Daniela O., 2016.* [52]

4.3.3. Sodium Valproate (Na-VPA)

Due to time constraints, it was not possible to expose both undifferentiated hSKPs and hSKPs HPC to Na-VPA. Therefore, only HepG2 were exposed for 72 hours to sub cytotoxic concentrations (0.05mM) of this compound.

The steatogenic effect of this compound in HepG2 cells is not evident (*Figure 4.12*).

In order to compare results and complete this study, the hSKPs with Na-VPA exposure must be made. In addition, Robim M. Rodrigues and his co-workers have already showed in 2015 that Na-VPA induces lipid accumulation in hSKP-HPC cells. [56]

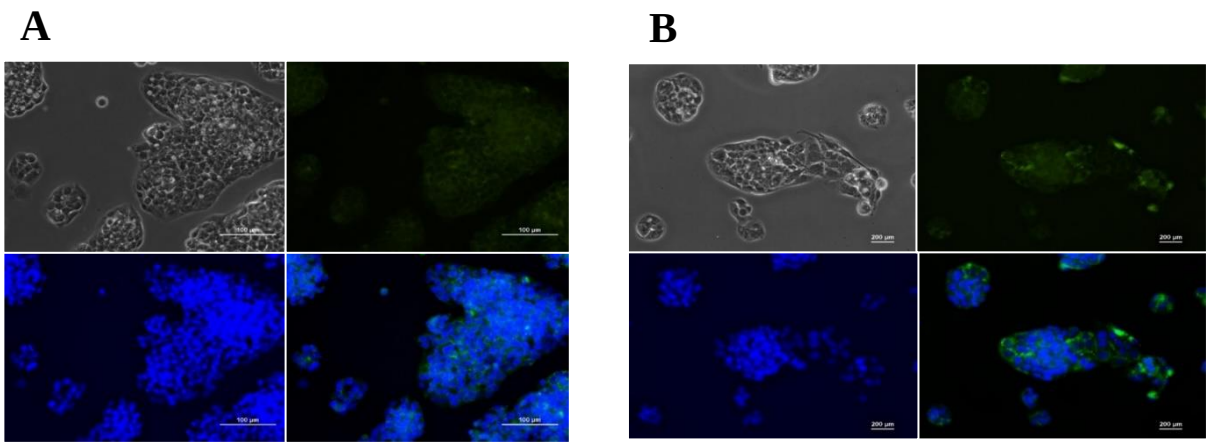

***Figure 4.12* – HepG2 treatment with sodium valproate.** HepG2 cytochemical neutral lipid staining after treatment with medium (control) **(A)** and 0.05mM Na-VPA **(B).** The pictures were obtained by fluorescence microscope with the 20× objective.

4.3.4. 2-Ethylhexanol (2-EH)

As determined by the cell viability assay, the concentration used to expose HepG2 for 72h to 2-EH was 1.25mM. On the other hand, previous studies indicated that the corresponding 2-EH IC_{10} value for undifferentiated hSKPs and hSKP-HPCs is 2.08mM.

In *Figure 4.14* we can observe that the treatment with the control *(Figure 4.13 A)* and with 2-EH *(Figure 4.13 B*) does not differ much from one another meaning that the accumulation of lipids is barely visible. The same happened with undifferentiated hSKP, the green dotted is not notorious which means that steatosis is not evident *(Figure 4.14 B*).

On the other hand, hSKP-HPC incubation with 2-EH showed an unexpected and significant cell death. However, the few viable cells (whose nucleus was coloured by DAPI) showed lipid accumulation *(Figure 4.15*).

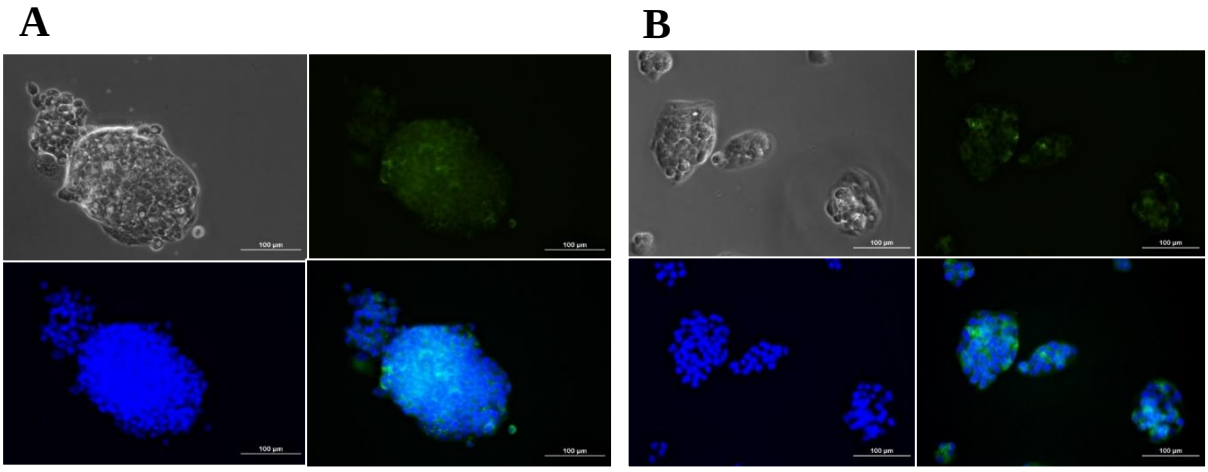

***Figure 4.13* –HepG2 treatment with 2-ethylhexanol.** HepG2 cytochemical neutral lipid staining after treatment with DMSO (control) **(A)** and 1.25mM 2-EH **(B).** The pictures were obtained by fluorescence microscope with the 20× objective.

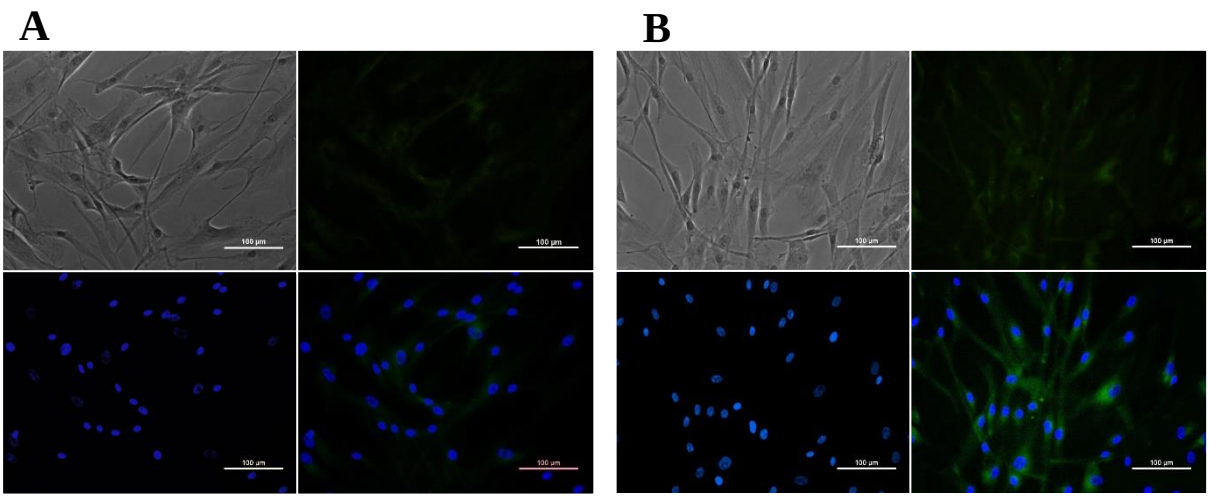

Figure 4.14 **- hSKPs treatment with 2-ethylhexanol.** Undifferentiated hSKPs cytochemical neutral lipid staining after treatment with DMSO and FBS (control) **(A)** and 2.08mM 2-EH **(B).** The pictures were obtained by fluorescence microscope with the 20× objective.

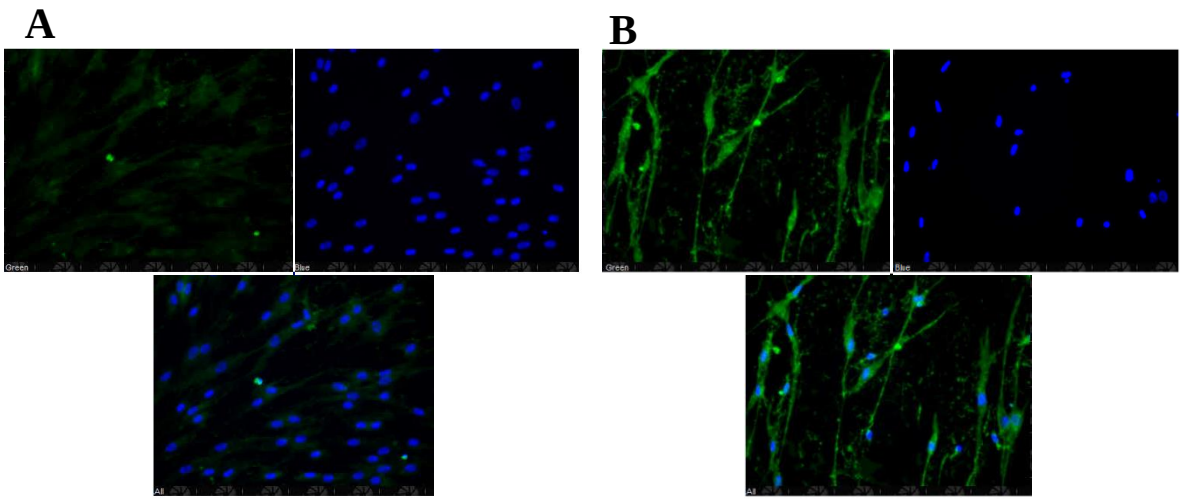

Figure 4.15 **– hSKP-HPC treatment with 2-ethylhexanol.** Differentiated hSKPs cytochemical neutral lipid staining after treatment with DMSO and FBS (control) **(A)** and 2.08mM 2-EH **(B).** The pictures were obtained by fluorescence microscope with the 20× objective. Adapted from *Costa, Daniela O., 2016.* [52]

4.4. Gene expression analysis

4.4.1. RNA extraction and cDNA production

As mentioned before, each condition (steatogenic compounds and controls) was tested in triplicate. After RNA isolation, measurements made by NanoDrop provided the information that is displayed on the tables below. Considering the RNA concentration of each sample, calculations were made to determine the amount of RNA (µL) that was necessary to have 0.5µg of RNA and the amount of water to perform a final volume of 30µL.

Nucleic acids and proteins have maximum absorbance at 260 and 280nm, respectively. The ratio of absorbances at these wavelengths has been used as a measure of the purity in nucleic acid extractions. A ratio of 2.0 is generally accepted as "pure" for RNA. Similarly, absorbance at 230nm is accepted as being the result of other contamination, therefore the ratio of A260/A230 for "pure" are commonly in the range of 2.0-2.2.

On each cell model, the levels of RNA purity were considered acceptable, the ratio A260/A230 was relatively near to 2.0 as result of absence of protein contamination. However, the rate A260/A230 was low which means that there is a contaminant absorbing at 230nm (usually products used in the extraction such as guanidine and phenol).

***Table 4.1* – RNA extraction table results for HepG2**. HepG2 RNA purity after extraction and respective RNA concentrations.

Sample	A260	A280	260/280	260/230	C RNA (ng/µl)	C RNA (µg/µl)	µl RNA (0.5 µg)	µL DEPC
Na-OA1	11.406	5.563	2.05	1.71	456.2	0.4562	1.1	28.9
Na-OA 2	13.263	6.375	2.08	1.61	530.5	0.5305	0.9	29.1
Na-OA 3	11.6	5.72	2.03	1.88	464	0.464	1.1	28.9
CTL1 1	14.458	6.841	2.11	1.98	578.3	0.5783	0.9	29.1
CTL1 2	17.259	8.087	2.13	1.81	690.3	0.6903	0.7	29.3
CTL1 3	15.967	7.686	2.08	1.93	638.7	0.6387	0.8	29.2
Tet 1	13.816	6.46	2.14	1.54	552.6	0.5526	0.9	29.1
Tet 2	14.494	6.8	2.13	1.94	579.7	0.5797	0.9	29.1
Tet 3	16.321	7.788	2.1	2.03	652.9	0.6529	0.8	29.2
CTL2 1	14.781	7.085	2.09	1.91	591.2	0.5912	0.9	29.2
CTL2 2	12.294	5.724	2.15	1.81	491.8	0.4918	1.0	29.0
CTL2 3	13.709	6.59	2.08	1.93	548.4	0.5484	0.9	29.1
Na-VPA 1	15.397	7.405	2.08	1.84	615.9	0.6159	0.8	29.2
Na-VPA 2	10.815	5.304	2.04	1.62	432.6	0.4326	1.2	28.8
Na-VPA 3	9.909	4.84	2.05	1.82	396.4	0.3964	1.3	28.7
CTL3 1	7.614	3.711	2.05	1.61	304.6	0.3046	1.6	28.4
CTL3 2	14.888	7.158	2.08	1.97	595.5	0.5955	0.8	29.2
CTL3 3	8.14	3.993	2.04	1.94	325.6	0.3256	1.5	28.5
2-EH 1	15.237	7.322	2.08	2.03	609.5	0.6095	0.8	29.2
2-EH 2	14.544	7.065	2.06	2.03	581.8	0.5818	0.9	29.1
2-EH 3	15.07	7.199	2.09	2.02	602.8	0.6028	0.8	29.2

***Table 4.2* – RNA extraction table results for hSKPs.** Undifferentiated hSKPs RNA purity after extraction and respective RNA concentrations.

Sample ID	A260	A280	260/280	260/230	C RNA (ng/µl)	C RNA (µg/µl)	µl RNA (0.5 µg)	µL DEPC
Tet 1	5.082	2.445	2.08	1.66	203.3	0.203	2.5	27.5
Tet 2	5.447	2.659	2.05	1.63	217.9	0.218	2.3	27.7
Tet 3	5.93	2.873	2.06	1.8	237.2	0.237	2.1	27.9
2-EH 1	3.767	1.843	2.04	1.9	150.7	0.151	3.3	26.7
2-EH 2	3.597	1.738	2.07	1.02	143.9	0.144	3.5	26.5
2-EH 3	3.669	1.787	2.05	1.54	146.8	0.147	3.4	26.6
Na-OA 1	1.55	0.783	1.98	1.29	62	0.062	8.1	21.9
Na-OA 2	1.146	0.578	1.98	1.11	45.8	0.046	10.9	19.1
Na-OA 3	1.435	0.721	1.99	1.49	57.4	0.057	8.7	21.3
CTL1 1	5.575	2.742	2.03	2.02	223	0.223	2.2	27.8
CTL1 2	5.023	2.431	2.07	1.78	200.9	0.201	2.5	27.5
CTL1 3	5.047	2.478	2.04	1.82	201.9	0.202	2.5	27.5

***Table 4.3* –RNA extraction table results for hSKP-HPC.** hSKPs HPC RNA purity after extraction and respective RNA concentrations.

Sample ID	A260	A280	260/280	260/230	C RNA (ng/µl)	C RNA (µg/µl)	µl RNA (0.5 µg)	µL DEPC
Tet 1	2.408	1.174	2.05	1.25	96.3	0.0963	5.2	24.8
Tet 2	1.519	0.747	2.08	0.34	60.8	0.0608	8.2	21.8
Tet 3	1.513	0.763	1.98	0.81	60.5	0.0605	8.3	21.7
2-EH 1	1.503	0.746	2.02	1.25	60.1	0.0601	8.3	21.7
2-EH 2	1.088	0.588	1.85	0.78	43.5	0.0435	11.5	18.5
2-EH 3	1.431	0.682	2.1	0.38	57.2	0.0572	8.7	21.3
Na-OA 1	2.215	1.114	1.99	1.1	88.6	0.0886	5.6	24.4
Na-OA 2	2.736	1.349	2.03	1.38	109.5	0.1095	4.6	25.4
Na-OA 3	1.795	0.887	2.02	0.36	71.8	0.0718	7.0	23.0
CTL1 1	1.891	0.927	2.04	0.96	75.6	0.0756	6.6	23.4
CTL1 2	1.785	0.901	1.98	1.21	71.4	0.0714	7.0	23.0
CTL1 3	2.359	1.164	2.03	1.41	94.4	0.0944	5.3	24.7

4.4.2. Selection of the housekeeping genes – geNorm

On each run, five housekeeping genes were used to normalize the gene expression. As showed on one of the graphics, the geNorm software calculates the gene-stability measure M and the lowest the value, the higher the expression stability. A gene with M value below 0.5 is generally accepted as an appropriate reference gene.

In addition, the pairwise variation Vn/n+1 (n=number of internal control genes in use) determines the possible need of including more genes for normalization. This function is represented on the second graphic and the considered cut-off value is 0,15, below which the additional control gene is not required.

4.4.2.1. HepG2 optimal reference target selection

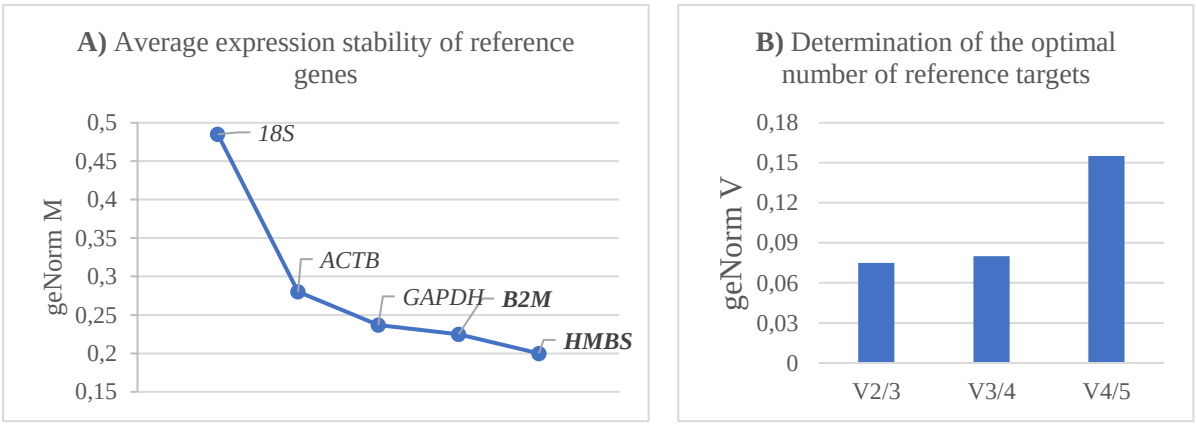

***Figure 4.16* – HepG2 optimal reference target selection**. HepG2 reference target stability analysis by calculation of geNorm M (A) and determination of the optimal number of reference targets by calculation of geNorm Vn/n+1.

By analysing *Figure 4.16 A)*, we can conclude that HepG2 housekeeping genes have high reference target stability (considered when average geNorm M ≤ 0.5) that is typically seen when evaluating candidate reference targets on a homogeneous set of samples.

According to *Figure 4.16 B)*, the optimal number of reference targets in this experimental situation is 2 (geNorm V < 0.15 when comparing a normalization factor based on the 2 or 3 most stable targets). As such, the optimal normalization factor was calculated as the geometric mean of reference targets *B2M* and *HMBS*.

4.4.2.2. Undifferentiated hSKP and hSKP-HPC optimal reference target selection

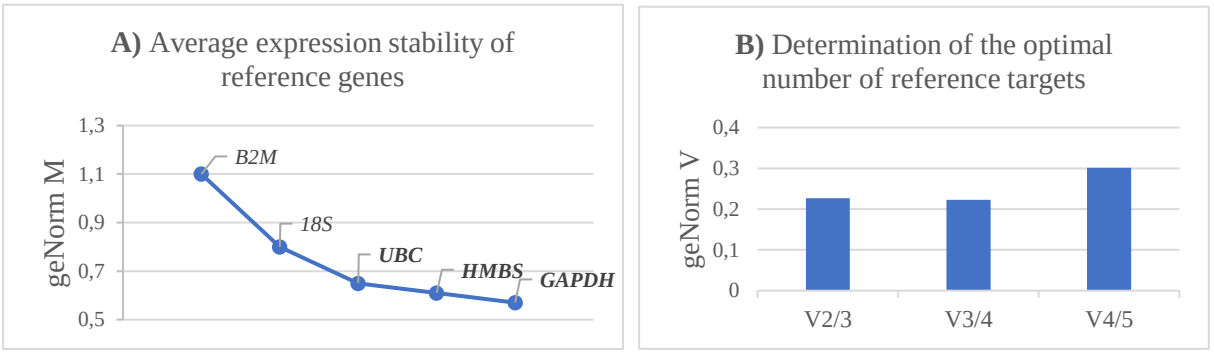

***Figure 4.17* – hSKP optimal reference target selection.** Undifferentiated hSKP reference target stability analysis by calculation of geNorm M (A) and determination of the optimal number of reference targets by calculation of geNorm Vn/n+1.

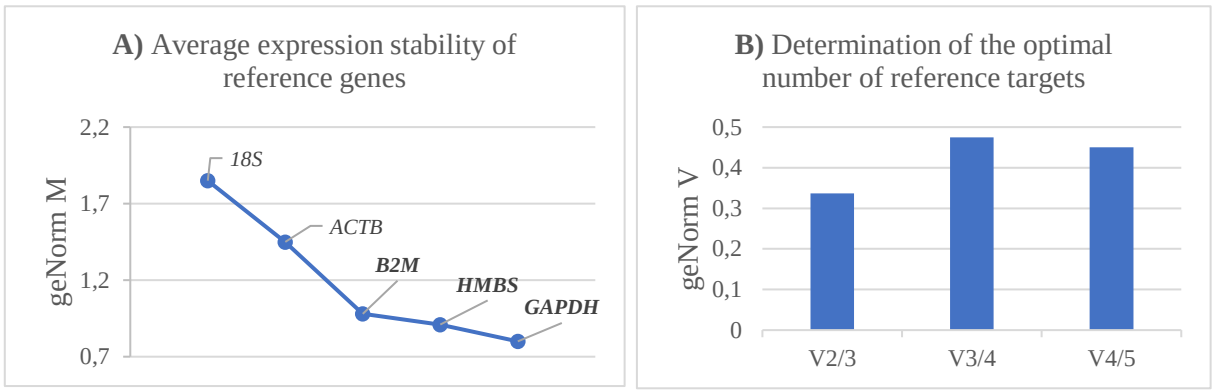

***Figure 4.18* – hSKP-HPC optimal reference target selection**. hSKP-HPC reference target stability analysis by calculation of geNorm M (A) and determination of the optimal number of reference targets by calculation of geNorm Vn/n+1.

By analysing *Figures 4.17 A)* and *4.18 A)*, we can infer that hSKPs (undifferentiated and HPC) housekeeping genes have medium reference target stability (0.5 < average geNorm M ≤ 1.0). This is typically seen when evaluating candidate reference targets on a heterogeneous set of samples.

For both undifferentiated hSKP *(Figure 4.17 B)* and hSKP-HPC *(Figure 4.18 B)*, no optimal number of reference targets could be determined, as the variability between sequential normalization factors (based on the n and n+1 least variable reference targets) is relatively high (geNorm V > 0.15). The ideal situation is to evaluate additional candidate reference targets however due to timing issues this was not possible. As an alternative, the 3 reference targets with lowest M value were used (*UBC*, *HMBS* and *GAPDH* for undifferentiated hSKP; *B2M*, *HMBS* and *GAPDH* for hSKP-HPC) as the use of multiple (non-optimal in this case) reference targets results in more accurate normalization compared to the use of a single non-validated reference target.

4.4.3. Gene expression analysis of steatosis-related genes

The induced steatosis was evaluated at a molecular level, through the analysis of the expression of genes involved in the molecular mechanisms of NAFLD: *CD36, FASN*, *SCD1*, *ACASB*, *CPT1A* and *APOB*[2]. These compounds may potentially induce steatosis through different mechanisms listed on *Table 4.4*.

***Table 4.4* – Genes of interest to the study.** Selection of genes and their respective involvement in the molecular pathway of NALFD.

Gene		Molecular mechanism involved
CD36	Cluster of differentiation 36	FA uptake
FASN	Fatty acid synthase	*De novo* lipogenesis
SCD1	Stearoyl-CoA desaturase 1	*De novo* lipogenesis
ACADSB	Short/branched chain acyl-CoA dehydrogenase	FA β – oxidation
CPT1A	Carnitine palmitoyltransferase 1A	FA β – oxidation
ApoB	Apolipoprotein B	TG secretion

After 24 hours of exposure with steatogenic compounds, the RNA was extracted as described above and the cDNA was prepared, cleaned-up and stored at -80ºC. Before starting the qPCR, a layout for each plate was designed and the amounts to prepare the standard series were calculated. The range of housekeeping genes used for each cell model was slightly different due to primers availability restrictions. Each exposure condition (steatogenic compounds and controls) was tested in triplicate on the same plate as showed above on the qPCR laytouts. In addition, each qPCR assay was perfomed twice meaning that every plate layout (for each cell model and for each primer) was tested in two different days.

In addition, only the results with differences above 1.5 fold-change were considered relevant for this study.

[2] The *APOB* gene was not included on qPCR results for undifferentiated hSKPs due to primer and time-related constraints.

4.4.3.1. Sodium Oleate

HepG2

HepG2 incubation with the fatty acid Na-OA led to a notable 6.33 fold decrease in *CPT1A* mRNA levels. CPT1A is responsible for FAs internalization in the mithocondria for β-oxidation. On the other hand, qPCR results reflect a slight decrease of *FASN* expression (-1.59), a gene that encodes a protein involved in FA synthesis.

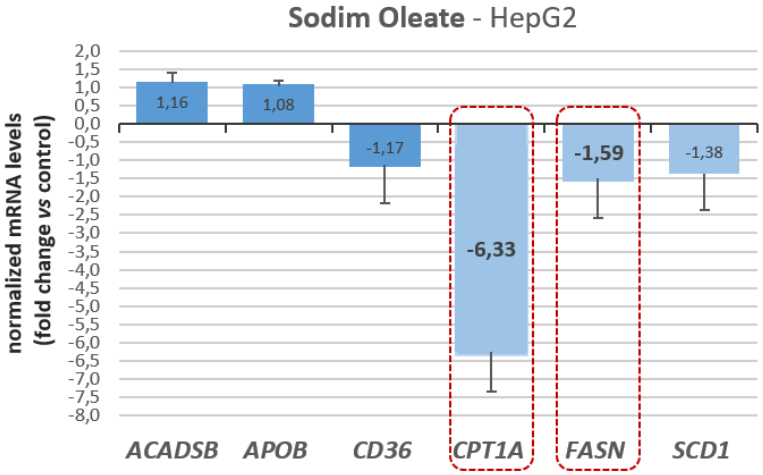

***Figure 4.19* – qPCR results for HepG2 exposure to 1mM of Sodium Oleate.** The present values are expressed as the fold change of $2^{-\Delta\Delta CT}$ and were normalized to two housekeeping genes (*B2M* and *HMBS*).

Undifferentiated hSKPs

hSKPs exposure to Na-OA led to a 2.41 fold increase in *CD36* mRNA levels. This gene encodes for a transmembrane transporter protein that facilitates the uptake and intracellular trafficking of FFA. Also, Na-OA slightly decreases the *CPT1A* expression (-1.58). Lastly, a 1.79 fold increased in *SCD1* mRNA expression was observed. *SCD1* is a protein involved in *de novo* lipogensis that will transform FA to TG.

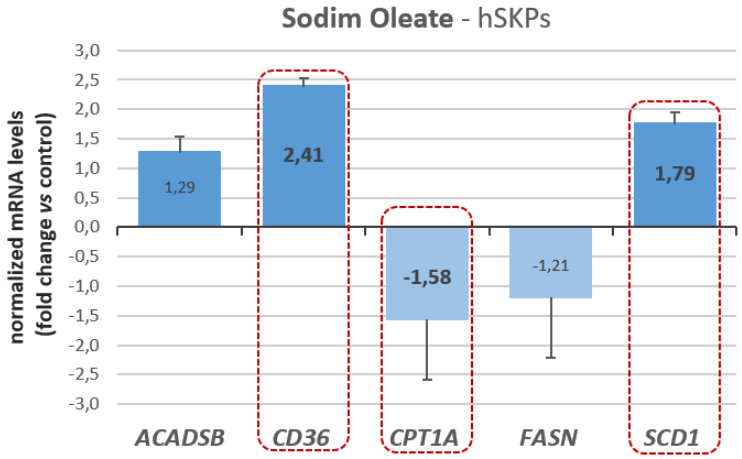

***Figure 4.20* – qPCR results for hSKPs exposure to 0.07mM of Sodium Oleate**. The present values are expressed as the fold change of $2^{-\Delta\Delta CT}$ and were normalized to two housekeeping genes *(UBC, HMBS* and *GAPDH).*

hSKP-HPC

The obtained results with hSKP-HPCs do not showed very relevant changes. Incubation with Na-OA led to a slight up-regulation of *APOB* mRNA levels (1.49), a protein involved in lipid secretion. In addition, an up-regulation of *CD36* mRNA levels (1.51) was observed.

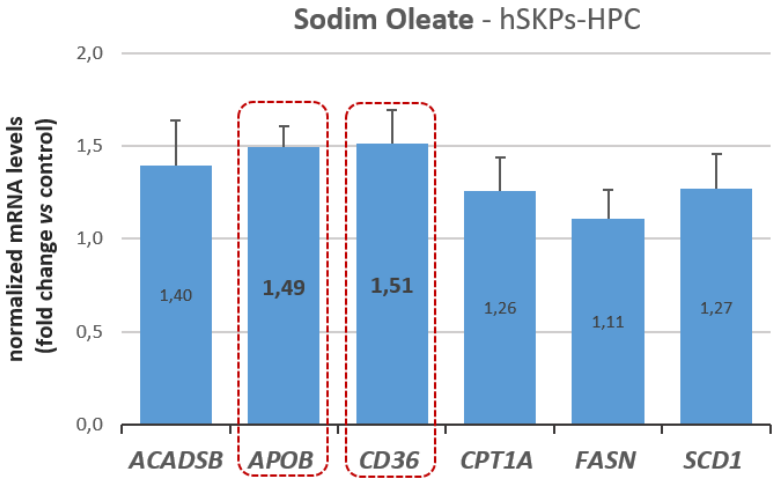

***Figure 4.21* – qPCR results for hSKP-HPCs exposure to 0.07mM of Sodium Oleate.** The present values are expressed as the fold change of $2^{-\Delta\Delta CT}$ and were normalized to two housekeeping genes *(B2M, HMBS* and *GAPDH).*

4.4.3.2. Tetracycline

HepG2

After 24h incubation with Tet, 1.85 fold decrease in *APOB* mRNA levels was detected. The genes *CPT1A* and *FASN* were also down-regulated, however, the fold changes were less significant (-1.48 and -1.51, respectively).

On the other hand, the *CD36* gene expression was slightly increased (1.51) which goes along with results obtained in previous studies. [24]

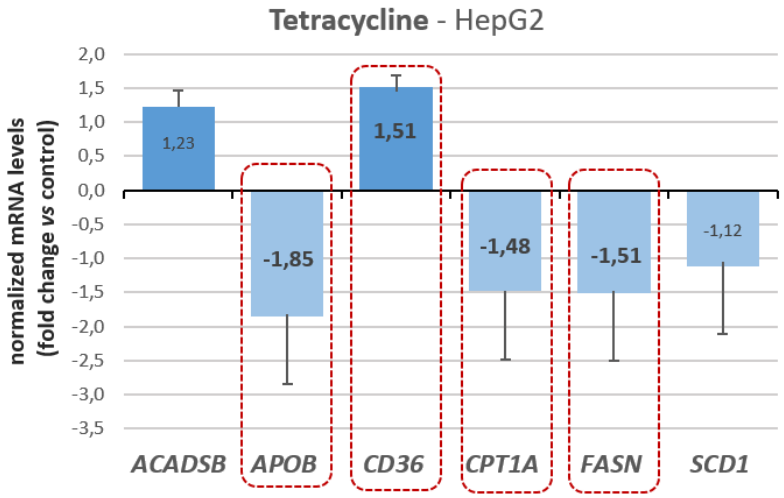

***Figure 4.22* – qPCR results for HepG2 exposure to 0.52mM of Tetracycline.** The present values are expressed as the fold change of $2^{-\Delta\Delta CT}$ and were normalized to two housekeeping genes (*B2M* and *HMBS*).

Undifferentiated hSKPs

hSKPs exposure to Tet resulted on a 2.11 fold increase in *CD36* mRNA levels. On the contrary, expressions of *FASN* and *SCD1*, genes involved in *de novo* lipogenesis, were down-regulated (2.22 and 3.67, respectively).

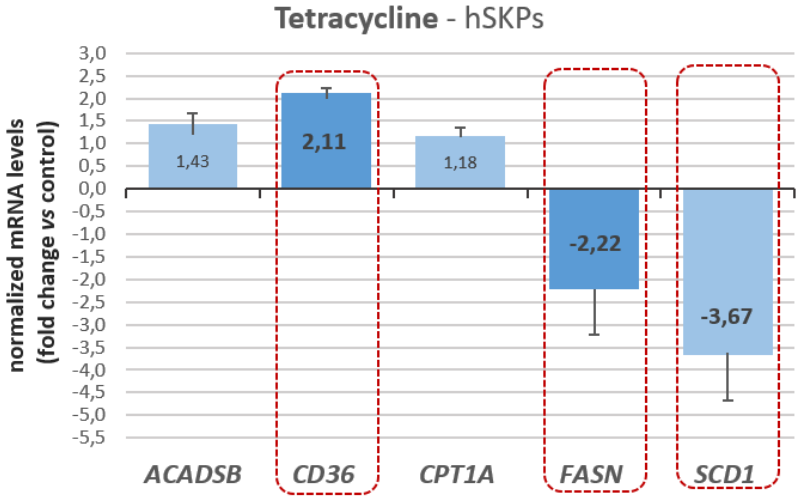

***Figure 4.23* – qPCR results for hSKPs exposure to 0.56mM of Tetracycline.** The present values are expressed as the fold change of $2^{-\Delta\Delta CT}$ and were normalized to two housekeeping genes *(UBC, HMBS* and *GAPDH).*

hSKP-HPC

As shown in *Figure 4.24*, the hSKP-HPCs exposure to Tet did not produce relevant and conclusive results.

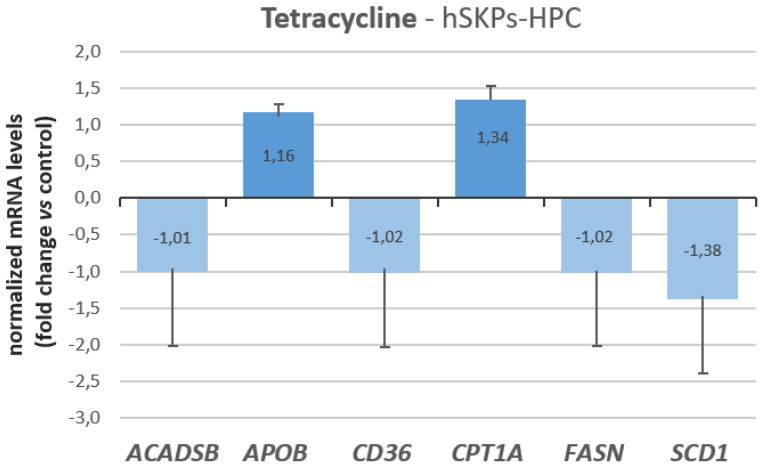

***Figure 4.24* – qPCR results for hSKP-HPCs exposure to 0.56mM of Tetracylcine.** The present values are expressed as the fold change of $2^{-\Delta\Delta CT}$ and were normalized to two housekeeping genes *(B2M, HMBS* and *GAPDH).*

4.4.3.3. Sodium Valproate

Once again, the qPCR results obtained in HepG2 cells treated with Na-VPA were not significant.

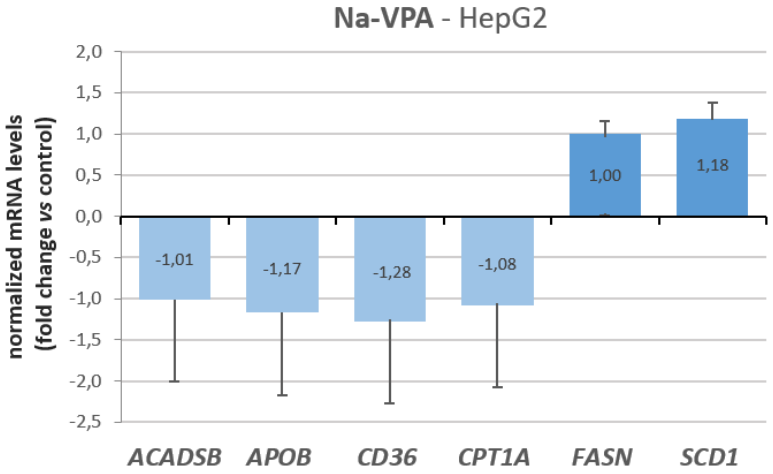

***Figure 4.25* – qPCR results for HepG2 exposure to 0.50mM of Sodium Valproate.** The present values are expressed as the fold change of $2^{-\Delta\Delta CT}$ and were normalized to two housekeeping genes (*B2M* and *HMBS).*

4.4.3.4. 2-Ethylhexanol

HepG2

HepG2 exposure to 2-EH lead to an up-regulation of all analized genes, however, the fold change values were not very significant. *SCD1* and *FASN* gene expression were increased (1.47 and 1.54, respectively). Also, *CD36* mRNA expression was slightly up-regulated (1.50) as well as *CPT1A* (1.50) mRNA expression.

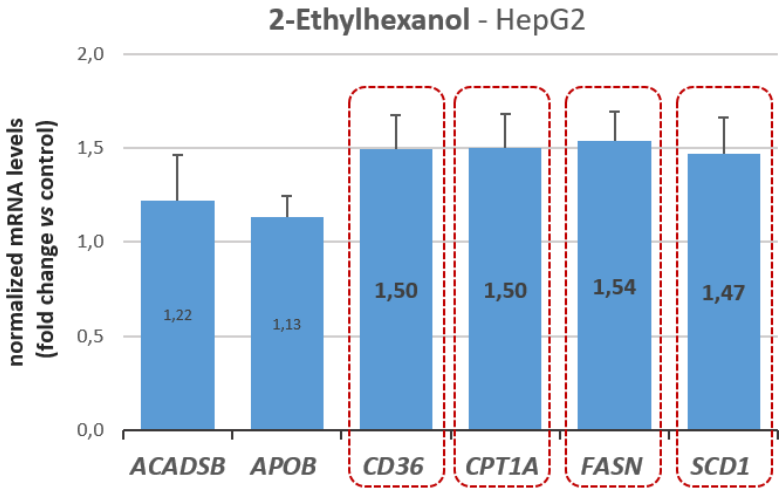

***Figure 4.26* – qPCR results for HepG2 exposure to 1.25mM of 2-ethylhexanol.** The present values are expressed as the fold change of $2^{-\Delta\Delta CT}$ and were normalized to two housekeeping genes (*B2M* and *HMBS).*

Undifferentiated hSKPs

Treatment of hSKPs with 2-EH lead to the 2.02 fold-increase in *CD36* transporter mRNA levels. In addition, a down-regulation was detected in *SCD1* expression (-1.55).

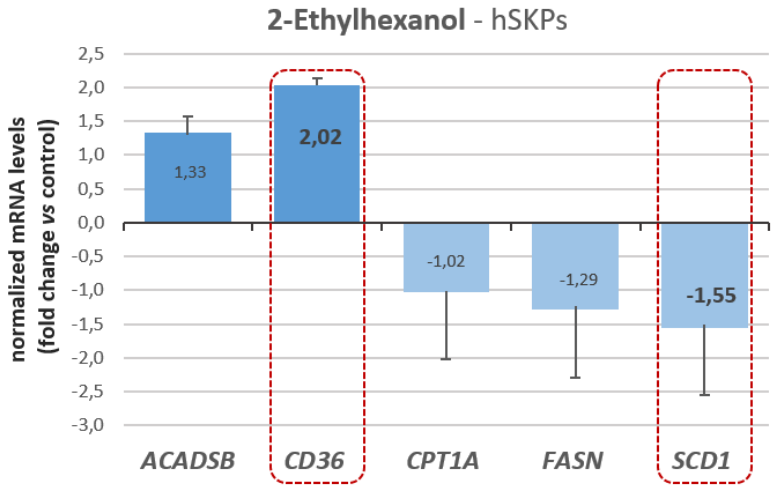

***Figure 4.27* – qPCR results for hSKPs exposure to 2.08mM of 2-ethylhexanol.** The present values are expressed as the fold change of $2^{-\Delta\Delta CT}$ and were normalized to two housekeeping genes *(UBC, HMBS* and *GAPDH).*

hSKP-HPC

hSKP-HPC exposure to 2-EH led to an up-regulation of *APOB* (1.94) and a down-regulation of *CD36* (-2.42). A less significant fold increase was observed in *SCD1* mRNA levels (1.50).

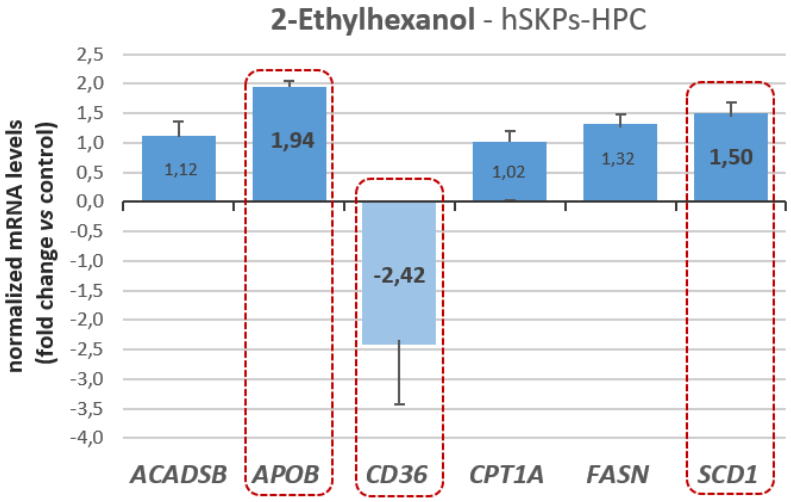

***Figure 4.28* – qPCR results for hSKP-HPCs exposure to 2.08mM of 2-thylhexanol**. The present values are expressed as the fold change of $2^{-\Delta\Delta CT}$ and were normalized to two housekeeping genes *(B2M, HMBS* and *GAPDH).*

5. Discussion

When considering the cytochemical staining results, HepG2 was the cell model that revealed lower sensitivity. The incubation with Na-VPA and 2-EH showed the less evident lipids accumulation. Therefore, and bearing in mind the inaccurate result of the 2-EH MTT assay, the determination of IC_{10} value should be recalculated considering that a higher value is expected. The same assay must be made for Na-VPA in order to determinate whether the IC_{10} employed was correct. The incubation with Na-OA led to a slight accumulation of lipids that was also present in the control which lead us to believe that FBS might induce steatosis as well. In addition, Tet was the compound that led to a higher accumulation of lipids on this cell model. Besides, a clear change in morphology was observed meaning that this compound has effects on other molecular pathways that we do not know.

When it comes to cytochemical staining of hSKPs, hSKP-HPC showed higher fluorescence than undifferentiated hSKP. Incubation with Na-OA and Tet revealed lipid accumulation that was more intensive with hSKP-HPC. Among the three steatogenic compounds incubated with undifferentiated hSKPs, 2-EH was the one whose lipid accumulation was less evident. The hSKP-HPC incubation with 2-EH showed a high level of dead cells which advise us, once again, to repeat the MTT assay.

The overall results obtained in qPCR were inconclusive. The obtained fold changes of the genes of interest were low and not significant ($p>0.05$). Also, there was a high variation between the repeats as indicated by the high standard deviation values.

Considering obtained results with HepG2, exposure with Na-OA led to a notable down regulation of *CPT1A* expression. Since this protein is involved in β-oxidation, further studies are mandatory to demonstrate if this compound is able to reduce this catabolic process and, consequently, induce steatosis in HepG2. As observed in cytochemical staining, the qPCR remaining results were not notorious.

Undifferentiated hSKP qPCR results showed the highest number of significant fold changes. The three compounds employed led to an up-regulation in *CD36* mRNA levels. Therefore, might be useful to evaluate whether FA uptake is increased and, if so, to confirm the cause of that mechanism that might be induced by the steatogenic compounds. In addition, the exposure with the Tet led to a decrease in both genes involved in *de novo* lipogenesis (*FASN* and *SCD1*).

This might mean that endogenous synthesis of FAs could be increased, due to a compensatory effect in which the accumulation of lipids inhibits the production of new triglycerides. However, further experiments should be performed.

Unfortunately, despite the hepatic differentiation process, hSKP-HPC cell model did not have significant fold changes in qPCR. Only 2-EH induced a small increase in *CD36* mRNA expression. Cytochemical staining results were more favourable because steatosis was evident, however, since those pictures were taken in another experience with a different donor, we cannot directly compare the results. [52]

In order to clarify the unsatisfying results obtained with hSKP (specially hSKP-HPC) and to exclude errors related with an incorrect technique, the experience was repeated with the same donor by professor Robim M. Rodrigues and his co-workers. The data was once again unclear which led us to believe that the intrinsic characteristics the donor chosen for these experiments might be responsible for the falling expectations despite the encouraging previous data with cells from different donors.

Different donors may originate variations in proliferation, morphology, differentiation capacity, response to stimuli such as growth factors and cytokines. Also, it should be clarified whether or not the multipotency of stem cells significantly depends on the donor's profile (age, lifestyle, health conditions, etc.). To perform robust comparative studies, experiences should be conducted to include several donors (ideally with different ages, sexes and ethnicities). [57]

To pursue the research on NAFLD molecular mechanisms and to address some hypotheses raised by present experiments, future work is needed involving studies to:

- re-evaluate subcytotoxicity concentrations of tested compounds and cell models
- obtain cytochemical staing data from the same experience (same donor)
- test different exposure times to each compound
- select more stable housekeeping genes for qPCR through geNorm
- expose both undifferentiated and differentiated hSKP to Na-VPA
- include *APOB* gene expression in undifferentiated hSKP qPCR
- include another assays to evaluate protein levels and activity
- include other cell models such as HepRG
- screen multiple hSKP donors for further experiments

6. Conclusion

Although toxicological research has been improving during the last decades, liver toxicity remains the leading cause for the discontinuation of drug candidates. Therefore, to decrease the attrition rate of new chemical entities is crucial to develop alternative methods, such as human cell-based *in vitro* hepatic models that could contribute to a better evaluation of the hepatotoxic potential of new drugs.

Steatosis, the abnormal hepatic accumulation of lipids, is one of the most common liver disorders and the most frequent cause of chronic liver disease. Steatosis development might be related with several factors such as: high fat diet, pharmaceutical drugs and chemical exposure. In turn, NAFLD, a reversible condition, is characterized by the presence of lipid droplets and can progress to severe hepatic injuries such as liver fibrosis, cirrhosis and HCC. Therefore, steatogenic screening is a crucial assay during pre-clinical drug development.

Cell systems for drug screening and hepatotoxicity testing such as HepG2 represent a valuable tool for toxicological research. Despite being widely employed, these cells have a much lower metabolic capacity compared to the gold standard *in vitro* hepatic model, primary hepatocytes. Recently, human stem cell-based *in vitro* tests, relying on human biological systems were also considered a novel and atractive *in vitro* system for predicting liver toxicity. Robim M. Rodrigues and his co-workers characterized hepatic differentiated hSKP that expressed relevant hepatic markers. In addition, it was demonstrated that hSKP-HPC respond to acetaminophen exposure in a comparable way to primary human hepatocytes in culture. It was also proved that the incubation of this cell model with Na-VPA, an epilepsy drug known to induce hepatic steatosis, led to lipid accumulation. [36] [56]

In general, the obtained results in this experience were inconclusive. hSKP-HPC was the cell model that presented highest lipid droplets accumulation in cytochemical staining. However, this method is only qualitative and the obtained data were not clear enough. Besides, as mentioned before, the hKSP-HPCs staining photos were taken in another experience which used a different donor. Therefore, the comparison of the several exposures might not be valid. Furthermore, the qPCR results were not significant, undifferentiated hSKPs was the cell model with the highest number of significant fold changes.

Despite the uncertain results for hSKP-HPC, previous data proved that these cells are a promissing human hepatic *in vitro* model. As mentioned above, the experiments carried out for this thesis had several limitations and further investigation in this area is still necessary.

It is crucial to standardise and harmonise the procedures to prevent intralaboratory variability as well as to select the most responsive donors. There are no doubts that stem cells technology has been growing steadily and has many advantages over other cellular and animal models. However, their application in toxicology is still limited and with issues yet to overcome such as the influence of the differentiation protocol on lipid metabolism. Neverthless, this group is making efforts to overcome this barriers and prove that hSKP-HPCs may serve as a promising human-relevant *in vitro* model that can be employed as an alternative for scarce primary hepatocytes to study hepatic lipid-metabolism related disorders.

7. Bibliography

1. Koo S. Nonalcoholic fatty liver disease : molecular mechanisms for the hepatic steatosis. Clin and Mol Hepatol 2013;19:210–5.
2. Hassan K, Bhalla V, El Regal ME, Hesham A-Kader H. Nonalcoholic fatty liver disease: A comprehensive review of a growing epidemic. World J Gastroenterol. 2014;20(34):12082–101.
3. Anderson N. Molecular Mechanisms and Therapeutic Targets in Steatosis and Steatohepatitis. Pharmacol Rev. 2008;60(3):311–57.
4. Machado M, Cortez-Pinto H. Non-alcoholic fatty liver disease and insulin resistance. Eur J Gastroenterol Hepatol. 2005; 17:823–6.
5. Kneeman JM, Misdraji J, Corey KE. Secondary causes of nonalcoholic fatty liver disease. Ther Adv Gastroenterol. 2012;5(3):199–207.
6. Bertot LC, Adams LA. The natural course of non-alcoholic fatty liver disease. Int J Mol Sci. 2016;17(5).
7. Rinella ME. Nonalcoholic Fatty Liver Disease. Jama. 2015;313(22):2263-73.
8. Than NN, Newsome PN. A concise review of non-alcoholic fatty liver disease. Atherosclerosis. 2015;239(1):192–202.
9. Adams LA, Angulo P, Lindor KD. Nonalcoholic fatty liver disease. CMAJ. 2005;172(7):899–905.
10. Buzzetti E, Pinzani M, Tsochatzis EA. The multiple-hit pathogenesis of non-alcoholic fatty liver disease (NAFLD). Metabolism. 2016;65(8):1038–48.
11. Houghton D, Stewart CJ, Day CP, Trenell M. Gut Microbiota and Lifestyle Interventions in NAFLD. Int. J. Mol. Sci. 2016;1–29.
12. Cernea S, Cahn A, Raz I. Pharmacological management of nonalcoholic fatty liver disease in type 2 diabetes. Expert Rev Clin Pharmacol. 2017;10(5):535–47.
13. Day CP, James OF. Steatohepatitis: A Tale of Two "'Hits'"? Gastroenterology 1998;114(4):842–5.
14. Kawano Y, Cohen DE. Mechanisms of hepatic triglyceride accumulation in non-alcoholic fatty liver disease. J Gastroenterol. 2013;48:434–41.
15. Romana F, Pecere S, Gasbarrini A. Physiology and pathophysiology of liver lipid metabolism. Expert Rev. Gastroenterol. Hepatol. 2015;1-13.
16. Donato MT, Gómez-Lechón MJ. Drug-induced Liver Steatosis and Phospholipidosis: Cell-Based Assays for Early Screening of Drug Candidates. Current Drug Metabolism. 2012;13:1160-73.
17. Guiu-jurado E, Porras JA, Auguet T. Molecular pathways in non-alcoholic fatty liver disease. Clinical and Experimental Gastroenterology. 2014; 4(7):221–39.
18. Fabbrini E, Sullivan S, Klein S. Obesity and Nonalcoholic Fatty Liver Disease: Biochemical, Metabolic and Clinical Implications. Hepathology. 2013;51(2):679–89.

19. Browning JD, Horton JD. Molecular mediators of hepatic steatosis and liver injury. J. Clin. Invest. 2004;114(2):147-152.

20. Ress C, Kaser S. Mechanisms of intrahepatic triglyceride accumulation. World J Gastroenterol. 2016;22(4):1664–73.

21. Moravcová A, Červinková Z, Kučera O, Mezera V, Rychtrmoc D, Lotková H. The Effect of Oleic and Palmitic Acid on Induction of Steatosis and Cytotoxicity on Rat Hepatocytes in Primary Culture. Physiol. Res. 2015;64(5):627-36.

22. Cui W, Chen SL, Hu K. Quantification and mechanisms of oleic acid-induced steatosis in HepG2 cells. Am J Transl Res. 2010;2(1):95–104.

23. Chopra I. Roberts M. Tetracycline Antibiotics : Mode of Action , Applications , Molecular Biology , and Epidemiology of Bacterial Resistance. Microbiology and molecular biology reviews. 2001;65(2):232–60.

24. Choi Y, Lee C, Lee K, Jung S, Lee B. Increased Hepatic Fatty Acid Uptake and Esterification Contribute to Tetracycline-Induced Steatosis in Mice. Toxicological sciences. 2015;145(2):273–82.

25. Donato MT, Martínez-Romero A, Jiménez N, Negro A, Herrera G, Castell J V, et al. Chemico-Biological Interactions Cytometric analysis for drug-induced steatosis in HepG2 cells. Chemico-Biological Interactions. 2009;181:417–23.

26. Morceau F, Dicato M, Diederich M. Molecular and Therapeutic Potential and Toxicity of Valproic Acid. Journal of Biomedicine and Biotechnology. 2010.

27. Dash A, Figler RA, Sanyal AJ, Wamhoff BR. Drug-induced steatohepatitis. Expert Opinion on Drug Metabolism & Toxicology 2017;1744-7607.

28. Chrus A, Sznajdrowska A, Materna K. 2-Ethylhexanol Derivatives as Nonionic Surfactants : Synthesis and Properties. J Surfact Deterg. 2016;155–64.

29. Badr MZ, Handler JA, Whittakers M, Kauffman FC, Thurman RG, Interactions between plasticizers and fatty acid metabolism in the perfused rat liver and *in vivo*. Biochemical Pharmacology. 1990;39(4):715–721.

30. Tonder JJ Van, Steenkamp V, Gulumian M. Pre-Clinical Assessment of the Potential Intrinsic Hepatotoxicity of Candidate Drugs. New Insights into Toxicity and Drug Testing. InTech. 2013

31. Chmp SWP. Non-Clinical Guideline on Drug-induced hepatotoxicity. EMEA. 2008.

32. Ballet F. Hepatotoxicity in drug development : detection , significance and solutions. Journal of Hepatology. 1997;(6):26–36.

33. Lecluyse EL, Witek RP, Andersen ME, Powers MJ, Lecluyse EL, Witek RP, et al. Organotypic liver culture models : Meeting current challenges in toxicity testing. Critical Reviews in Toxicology. 2012;42(6):501-548.

34. Soldatow VY, LeCluyse EL, Griffith LG, Rusyn I. In vitro models for liver toxicity testing. Toxicol Res. 2014;2(1):23–39.

35. Faqi AS. A Comprehensive Guide to Toxicology in Preclinical Drug Development. International Journal of Toxicology. 2017;36(5):410-6.

36. Rodrigues RM, Kock J De, Branson S, Vinken M, Chaudhari U, Sachinidis A, et al. Human Skin-Derived Stem Cells as a Novel Cell Source for In Vitro Hepatotoxicity Screening of Pharmaceuticals. Stem Cells and Development. 2014;23(1).

37. Chavez-Tapia NC, Tiribelli C. In Vitro Models for the Study of Non-Alcoholic Fatty Liver Disease. Current Medicinal Chemistry. 2011;18:1079-84.

38. Dulak J, Szade K, Szade A, Nowak W, Józkowicz A. Adult stem cells : hopes and hypes of regenerative medicine. Acta Biochimica Polonica. 2015;62(3):329–37.

39. Biswas A, Hutchins R. Embryonic Stem Cells. Stem Cells and Development 2007;16:213–21.

40. Greenhough S, Medine CN, Hay DC. Pluripotent stem cell derived hepatocyte like cells and their potential in toxicity screening. Toxicology. 2010;278:250–5.

41. Kock J De, Rodrigues RM, Bolleyn J, Vanhaecke T, Rogiers V. Focus on Stem Cells as Sources of Human Target Cells for In Vitro Research and Testing. Altex Proceedings. 2007;4:541–8.

42. Yamanaka S. Perspective Induced Pluripotent Stem Cells : Past , Present , and Future. Cell Stem Cell. 2012;10(6):678–84.

43. Guguen-guillouzo C, Corlu A, Guillouzo A. Stem cell-derived hepatocytes and their use in toxicology. Toxicology. 2010;270:3–9.

44. Snykers S, Kock J De, Rogiers V, Vanhaecke. In Vitro Differentiation of Embryonic and Adult Stem Cells into Hepatocytes : State of the Art. Stem Cells. 2009;27:577–605.

45. Zuk PA, Zhu M, Ashjian P, Ugarte DA De, Huang JI, Mizuno H, et al. Human Adipose Tissue Is a Source of Multipotent Stem Cells. Molecular Biology of the Cell. 2002;13:4279–95.

46. Toma JG, Akhavan M, Fernandes KJL, Barnabé-heider F, Sadikot A, Kaplan DR, et al. Isolation of multipotent adult stem cells from the dermis of mammalian skin. Nature Cell Biology. 2001;3.

47. Dalgetty DM, Medine CN, Iredale JP, Hay DC. Progress and future challenges in stem cell-derived liver technologies. Am J Physiol Gastrointest Liver Physiol. 2009;297:241-8.

48. Biernaskie J a, McKenzie I a, Toma JG, Miller FD. Isolation of skin-derived precursors (SKPs) and differentiation and enrichment of their Schwann cell progeny. Nat Protoc. 2006;1(6):2803–12.

49. De Kock J, Vanhaecke T, Biernaskie J, Rogiers V, Snykers S. Characterization and hepatic differentiation of skin-derived precursors from adult foreskin by sequential exposure to hepatogenic cytokines and growth factors reflecting liver development. Toxicol Lett. 2009;23(8):1522–7.

50. Rodrigues RM, Heymans A, De Boe V, Sachinidis A, Chaudhari U, Govaere O, et al. Toxicogenomics-based prediction of acetaminophen-induced liver injury using human hepatic cell systems. Toxicol Lett. 2016;240(1):50–9.

51. Riss TL, Moravec RA, Niles AL, Benink HA, Worzella TJ, Minor L. Cell viability assays. Assay Guidance Manual. 2015;1–31.

52. Costa DF de O. Hepatic differentiation of skin-derived stem cells and their application within in vitro toxicity testing. Tese de Mestrado Integrado. Vrije Universiteit Brussel and Faculdade de Farmácia - Universidade de Lisboa; 2016.

53. Peirson SN, Butler JN. Quantitative polymerase chain reaction. Methods Mol Biol. 2007;362(2):349–62.

54. Bonab MM, Alimoghaddam K, Talebian F, Ghaffari SH, Ghavamzadeh A, Nikbin B, et al. Real-time PCR handbook. Lab Chip. 2015;4(2):189–200.

55. Vandesompele J, De Preter K, Pattyn F, Poppe B, Van Roy N, De Paepe A, et al. Accurate normalization of real-time quantitative RT-PCR data by geometric averaging of multiple internal control genes. Genome Biol. 2002;3(7)

56. Rodrigues RM, Branson S, Boe V De, Vanhaecke T. In vitro assessment of drug - induced liver steatosis based on human dermal stem cell - derived hepatic cells. Arch Toxicol. 2016;90(3):677-89.

57. Heathman TRJ, Rafiq QA, Chan AKC, Coopman K, Nienow AW, Kara B, et al. Characterization of human mesenchymal stem cells from multiple donors and the implications for large scale bioprocess development. Biochem Eng J. 2016;108:14–23.